May 16, 2025

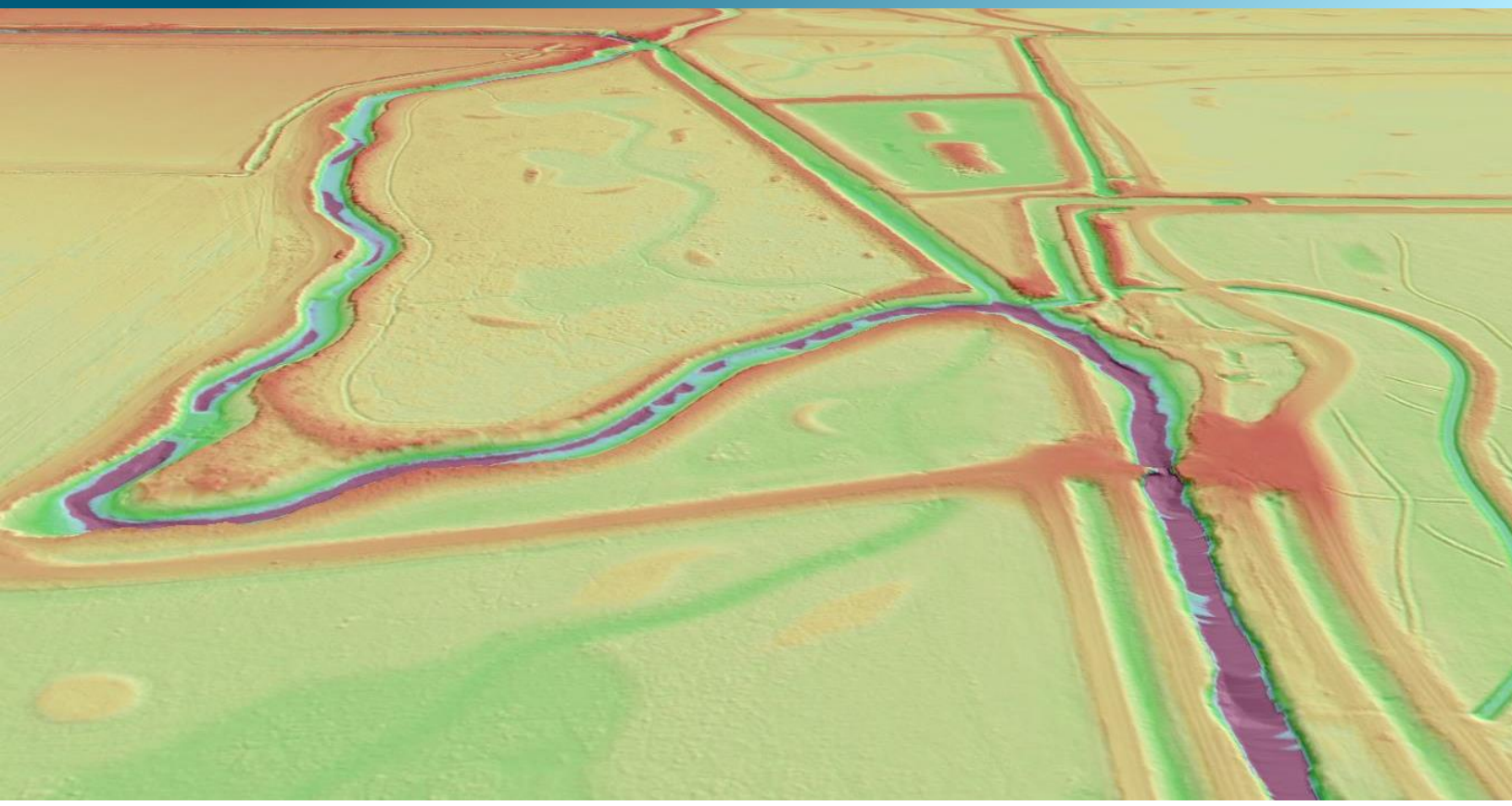

Putah Creek, Solano County, California

2025 Topobathymetric Lidar & Imagery Technical Report

Prepared For:

Solano County Water Agency

Solano County Water Agency
810 Vaca Valley Parkway
Suite 202
Vacaville, CA 95688

Prepared By:

NV5
1100 NE Circle Blvd, Ste. 126
Corvallis, OR 97330
PH: 541-752-1204

TABLE OF CONTENTS

Cover Photo: An oblique view looking west towards Putah Creek from the Yolo Bypass Wildlife Area in California. The 3D image was created from the lidar bare earth model symbolized by elevation.

LIST OF FIGURES

List of Tables

INTRODUCTION

This image was created from the Putah Creek topobathymetric lidar bare earth model symbolized by elevation and focused on an area where the creek has deep pools of water.

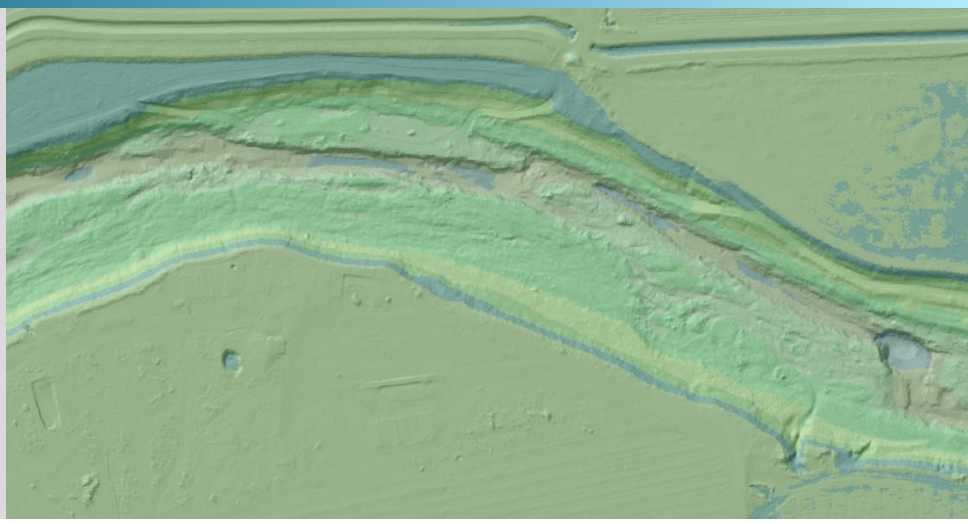

In January 2025, NV5 was contracted by the Solano County Water Agency (SCWA) to collect Topobathymetric Light Detection and Ranging (lidar) data and digital imagery in the winter of 2025 for the Putah Creek site in California. The Putah Creek project area of interest (AOI) covers the Monticello Dam at Lake Berryessa in the west and traverses Putah Creek eastward down through the valley to the ponds in the Yolo Bypass Wildlife Area to the southeast of the city of Sacramento; it also encompasses much of Old Canyon Creek and the Pleasant Creek tributaries. Traditional near-infrared (NIR) lidar was fully integrated with green wavelength return (bathymetric) lidar data in order to provide a seamless topobathymetric lidar dataset. Data were collected to aid SCWA in assessing the channel morphology and topobathymetric surface of the study area to support various research and activities along the Putah Creek.

This report accompanies the delivered topobathymetric lidar data and imagery, and documents contract specifications, data acquisition procedures, processing methods, and analysis of the final dataset including lidar accuracy, depth penetration, and density. Acquisition dates and acreage are shown in Table 1, a complete list of contracted deliverables provided to SCWA is shown in Table 3 with the coordinate reference system information for these deliverables shown in Table 2, and the project extent is shown in Figure 1.

Table 1: Acquisition dates, acreage, and data types collected on the Putah Creek site.

Project Site	Contracted Acres	Buffered Acres	Aerial Acquisition Dates	Data Type
Putah Creek, California	10,190	10,952	1/28/2025 – 1/30/2025, 2/27/2025	Topobathymetric Lidar
Putah Creek, California	10,190	6,855*	1/28/2025 – 1/30/2025	4 Band (RGBNIR) Digital Imagery

*Remaining imagery to be delivered at a later date

Deliverable Products

Table 2: Deliverable product coordinate reference system information.

Projection	Horizontal Datum	Vertical Datum	Units
California State Plane Zone 2	NAD83(2011)	NAVD88(GEOID18)	US Survey Feet

Table 3: Lidar and imagery products delivered for the Putah Creek project.

Product Type	File Type	Product Details
Points	LAS v.1.4 (*.las)	• All Classified Returns
Rasters	1.5 foot GeoTIFFs (*.tif)	• Void-Interpolated Topobathymetric Bare Earth Digital Elevation Models (DEM) • Void-Clipped Topobathymetric Bare Earth Digital Elevation Models (DEM) • Highest Hit Digital Surface Models (DSM) • Relative Elevation Model (REM) Mosaic • Intensity Images
Vectors	Shapefiles (*.shp)	• Boundary • Tile Index • Ground Survey Data • Bathymetric Coverage • Water's Edge Breaklines • Residual Pools
Digital Imagery	0.25 foot GeoTIFFs (*.tif)	• Tiled Imagery Mosaics
Digital Imagery	0.25 foot MrSID (*.sid)	• AOI Imagery Mosaic
Metadata	Extensible Markup Language (*.xml)	• Metadata
Reports	Adobe Acrobat (*.pdf)	• Lidar & Imagery Technical Data Report

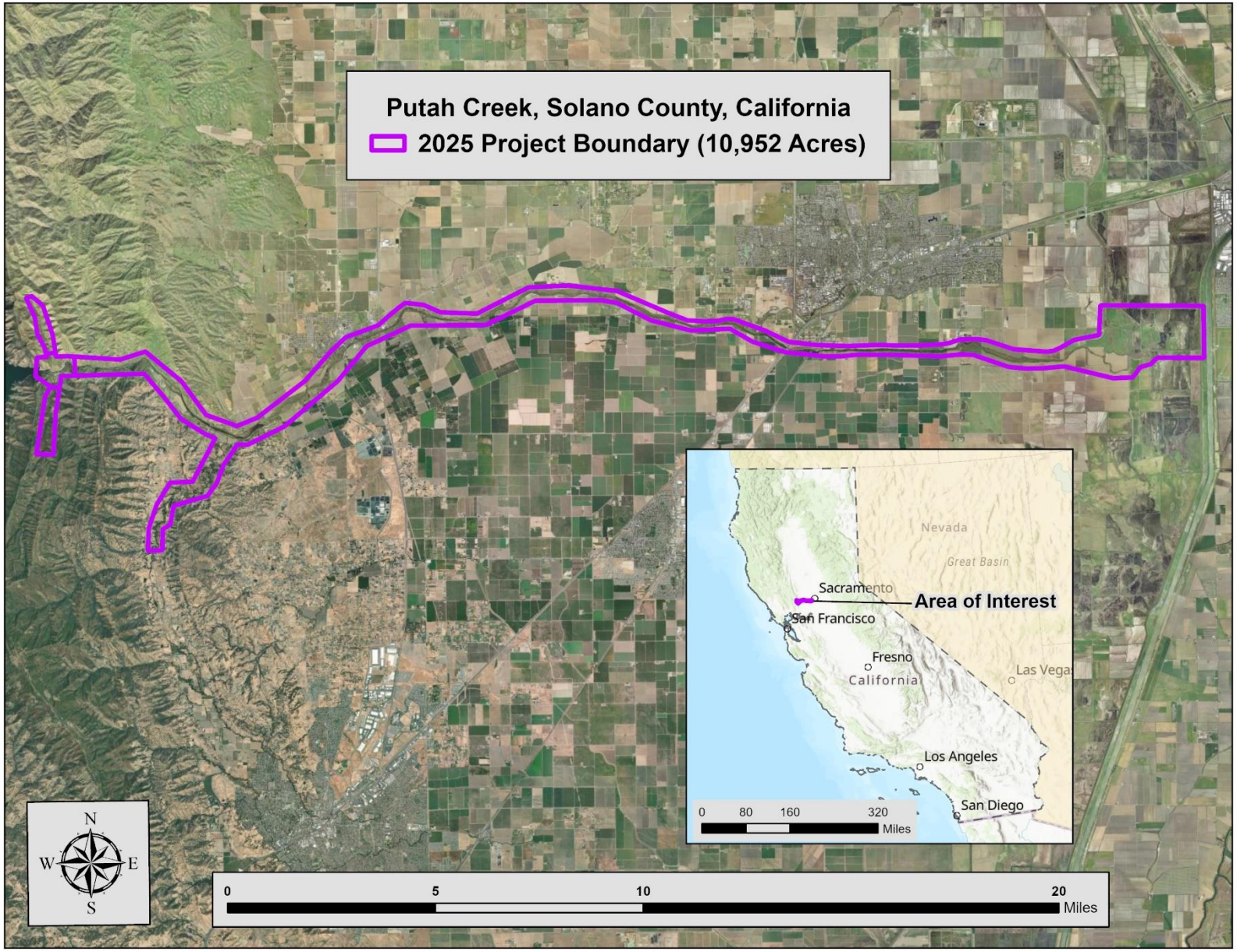

Figure 1: Location map of the Putah Creek site in California.

ACQUISITION

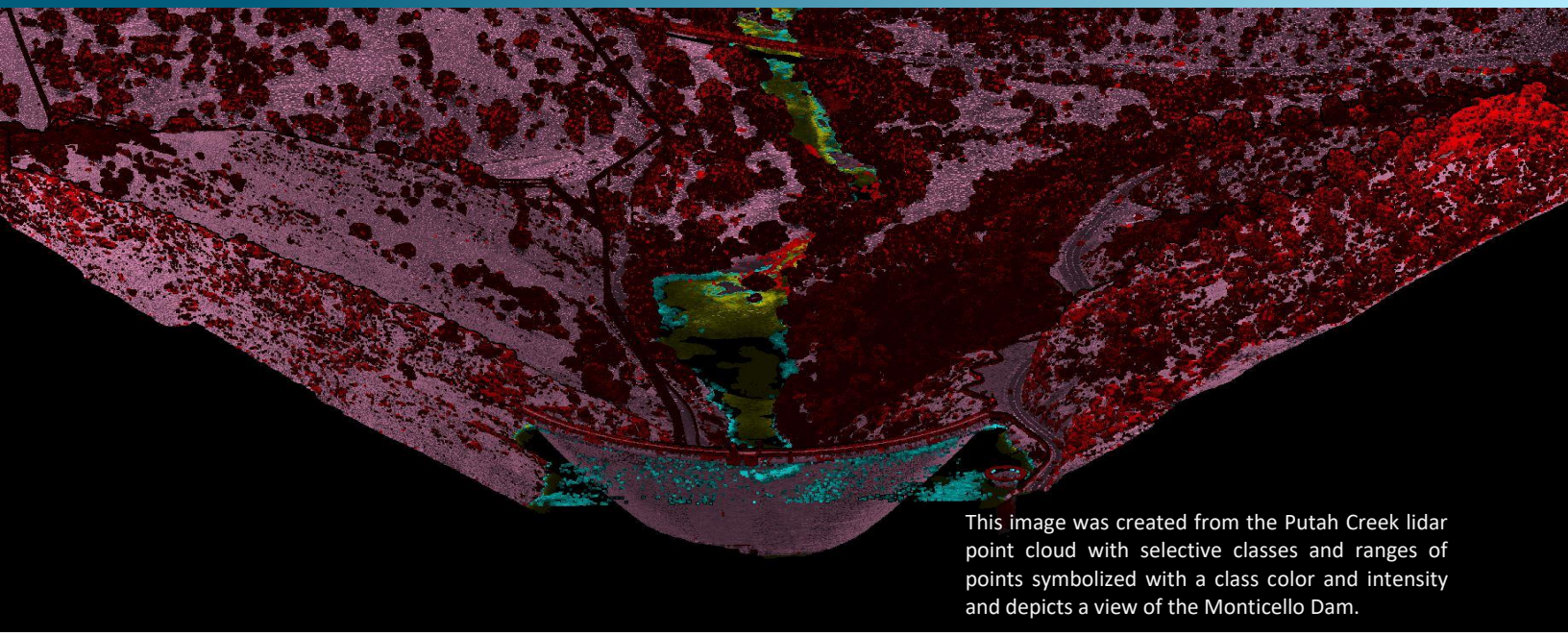

This image was created from the Putah Creek lidar point cloud with selective classes and ranges of points symbolized with a class color and intensity and depicts a view of the Monticello Dam.

Planning

In preparation for data collection, NV5 reviewed the project area and developed a specialized flight plan to ensure complete coverage of the Putah Creek study area at the target combined point density of ≥8 points/m^2 (0.74 points/ft^2). Acquisition parameters including orientation relative to terrain, flight altitude, pulse rate, scan angle, and ground speed were adapted to optimize flight paths and flight times while meeting all contract specifications. Figure 6 shows these optimized flight paths and dates.

Factors such as satellite constellation availability and weather windows must be considered during the planning stage. Any weather hazards or conditions affecting the flight were continuously monitored due to their potential impact on the daily success of airborne and ground operations. In addition, logistical considerations including private property access, potential air space restrictions, water levels (Figure 2), channel flow rates (Figure 3), and water clarity (Figure 4, Figure 5) were reviewed.

Turbidity Measurements and Secchi Depth Readings

In order to assess water clarity conditions prior to and during lidar and digital imagery collection, NV5 collected turbidity measurements and Secchi depth readings. Readings were collected at ten locations throughout the project site between January 28 and January 30, 2025. Turbidity observations were recorded three times to confirm measurements. Winds were noted to be calm at all site locations. Table 4 below provides turbidity and Secchi depth results per site on each day of data collection. A true Secchi depth reading is where the Secchi depth reaches extinction. However, because of shallow waters, safety concerns, and accessibility, all Secchi depth readings were noted to have reached the bottom surface of the creek bed (Table 4). Water levels at three designated water level stations were also recorded (Figure 4 and Table 5) as well as water clarity and stream observations (Figure 5).

Table 4: 2025 Putah Creek water clarity observations.

Date	Time (PST -8h)	Location	Latitude	Longitude	Turbidity Read 1 (NTU)	Turbidity Read 2 (NTU)	Turbidity Read 3 (NTU)	Secchi Depth (m)
1/28	1400	Site_2B Fishing access #1	38° 30' 51.47391"	-122° 04' 39.54692"	2.68	2.77	3.32	*> 0.8, easily visible at river bottom
1/29	1315	Site_1 at Pleasant Creek bridge	38° 28' 51.81169"	-122° 01' 40.01921"	1.79	1.74	1.76	*> 1.2, easily visible at river bottom
1/29	1320	Site_2 downstream of dam	38° 30' 47.32095"	-122° 05' 45.84992"	2.24	3.49	3.36	*> 0.6, easily visible at river bottom
1/29	1615	Site_3 access near Winters	38° 31' 21.68453"	-121° 57' 47.82011"	2.01	1.73	1.87	*> 0.7, easily visible at river bottom
1/29	1130	Site_5 at Solano Lake campground	38° 29' 42.86970"	-122° 01' 57.94707"	3.25	2.85	2.59	*> 0.3, easily visible at river bottom
1/29	1530	Site_6 near bridge	38° 31' 36.34183"	-121° 48' 14.01578"	1.74	2.05	1.71	*> 0.8, easily visible at river bottom
1/30	1130	Site_4 near Davis	38° 31' 23.75703"	-121° 46' 57.16296"	3.38	3.23	3.27	*> 1.4, barely visible at river bottom
1/30	1345	Site_7 near confluence	38° 30' 56.70174"	-121° 36' 40.64426"	5.80	5.92	6.71	*> 1.4, barely visible at river bottom
1/30	1210	Site_8 near UC Davis	38° 31' 01.61568"	-121° 45' 23.40343"	3.29	3.72	3.29	*> 1.1, easily visible at river bottom
1/30	1636	Site_9 near Davis	38° 31' 07.71931"	-121° 41' 33.87764"	2.29	2.45	2.44	NA, too shallow and muddy

** Measurement is depth to the bottom surface due to observational depth limitations*

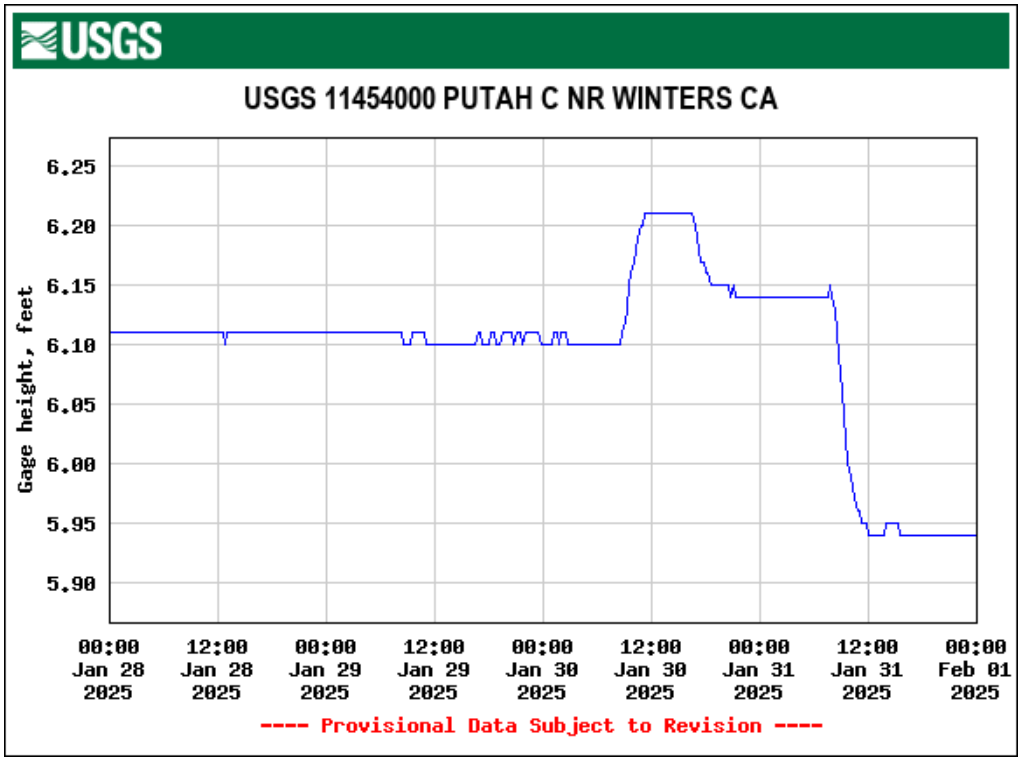

Figure 2: USGS Station 11454000 gage height along the Putah Creek at the time of lidar acquisition.

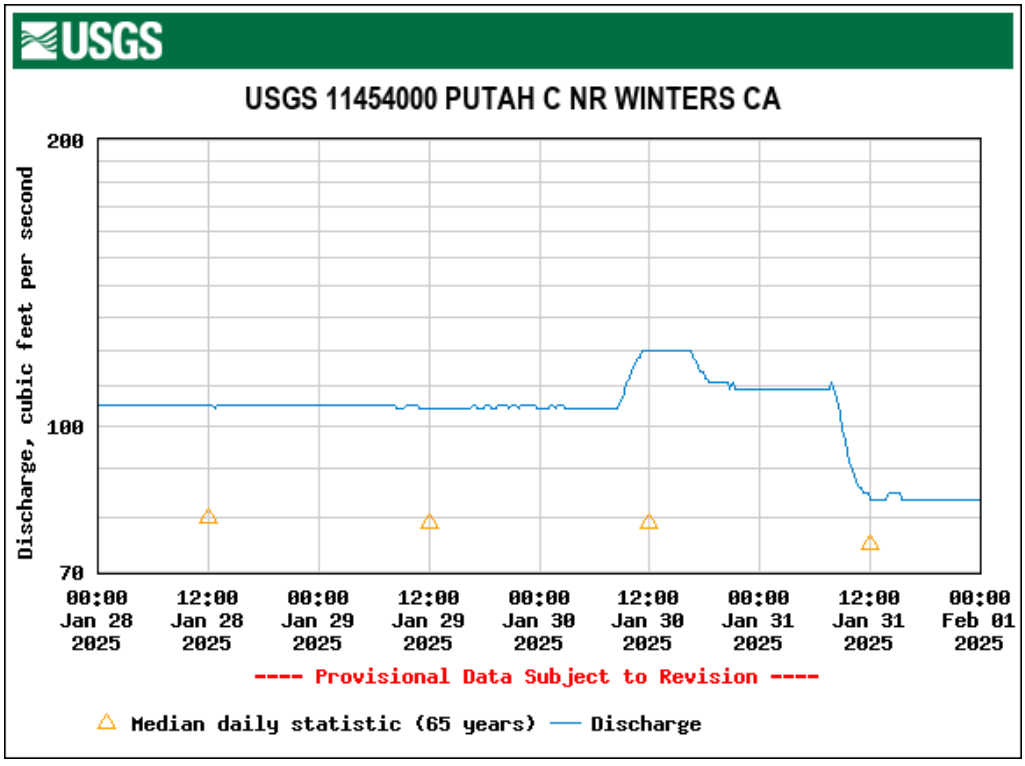

Figure 3: USGS Station 11454000 flow rates along the Putah Creek at the time of lidar acquisition.

Figure 4: Photos taken by NV5 acquisition staff show the three water level stations; the I-80 Station (above), I-505 Station (top right), and the Lo Rios Dam Station (right).

Table 5: Survey of water level and stage at three flow monitoring stations on Putah Creek on January 29 and 30, 2025. Projection is California State Plane Zone 2, horizontal datum is NAD83(2011), and vertical datum is NAVD88(Geoid18). Measurements are in US Survey Feet.

Date	Time (PST -8h)	Water Level Station	Stage at Staff Plate (Feet)	Water Level Elevation as Surveyed (Feet)	Easting (X)	Northing (Y)
1/29	1221	I-505 Station	4.82	93.881	6575215.434	1953298.104
1/30	1541	I-80 Station	5.56	31.398	6627090.718	1950549.243
1/30	1351	Los Rios Dam Station (Downstream Staff Plate)	2.96	8.041	6672903.436	1949897.342

Note: Water level elevation was collected using Survey-Grade GPS. The data was post-processed and exported into the spatial reference system listed above. The X and Y coordinates listed reference the location where the water level elevation was surveyed.

Figure 5: These photos taken by NV5 acquisition staff display water clarity conditions and submerged vegetation (left) and muck (right) on the creek bed at two locations within the Putah Creek site.

Airborne Lidar Survey

The lidar survey was collected using a Leica Chiroptera 5X (CH5X) green laser system mounted in a Cessna Grand Caravan. The CH5X performs well in both shallow and deep waters with dynamic surfaces, and automatically corrects for water refraction, making it useful in collecting riverine data. The CH5X system detects obstructions, such as vegetation and anthropogenic features with oblique lidar. This means it can provide additional information from multiple positions that more closely resembles the actual features and allows for more analyses than traditional imagery. This system provides a seamless integration between the NIR and Green channels.

The CH5X system acquires full waveform data for every pulse; however, a maximum of 15 returns can be stored due to LAS v1.4 file limitations. The recorded waveform enables range measurements for all discernible targets for a given pulse. The typical number of returns digitized from a single pulse range from 1 to 4 in the Putah Creek project dataset. It is not uncommon for some types of surfaces (e.g., dense vegetation or water) to return fewer pulses to the lidar sensor than the laser originally emitted. The discrepancy between first return and overall delivered density will vary depending on terrain, land cover, and the prevalence of water bodies. All discernible laser returns were processed for the output dataset. Table 6 summarizes the settings used to yield an average pulse density of at least 8 pulses/m^2 over the Putah Creek project area. Figure 6 shows the flightlines acquired using these lidar specifications.

NV5 detected topographic areas that were not meeting the density requirements. The areas were due to changes in terrain over the mountain ridges in the western section of the AOI. NV5 mobilized a 'refly' mission and collected additional lidar using a Riegl VQ-1560ii-S system on February 27, 2025. The Riegl VQ-1560ii-S laser system is equipped with an NIR sensor and can record unlimited range measurements (returns) per pulse. The settings used for this additional mission are also included in Table 6, and the location of the flights are presented in Figure 6.

All areas were surveyed with an opposing flight line side-lap of ≥70% (≥100% overlap) in order to reduce laser shadowing and increase surface laser painting. To accurately solve for laser point position (geographic coordinates x, y, and z), the positional coordinates of the airborne sensor and the orientation of the aircraft to the horizon (attitude) were recorded continuously throughout the lidar data collection mission. Position of the aircraft was measured twice per second (2 Hz) by an onboard differential GPS unit, and aircraft attitude was measured 200 times per second (200 Hz) as pitch, roll, and yaw (heading) from an onboard inertial measurement unit (IMU). To allow for post-processing correction and calibration, aircraft and sensor position and attitude data are indexed by GPS time.

Table 6: Lidar specifications and aerial survey settings.

Parameter	NIR Sensor	Shallow Green Sensor	NIR Sensor (Refly)
Acquisition Dates	1/28/2025 – 1/30/2025	1/28/2025 – 1/30/2025	2/27/2025
Aircraft Used	Cessna Grand Caravan	Cessna Grand Caravan	Cessna Grand Caravan
Sensor	Leica Chiroptera 5X	Leica Chiroptera 5X	Riegl VQ-1560ii-S
Laser Channel	NIR	Green	NIR
Maximum Returns	4	5	7
Resolution/Density	Average 8 points/m²	Average 8 points/m²	Average 8 points/m²
Nominal Pulse Spacing	0.35 m	0.35 m	0.35 m
Survey Altitude (AGL)	400 - 600 m	400 - 600 m	2532 m
Survey speed	145 knots	145 knots	145 knots
Field of View	40°	40°	58.5°
Mirror Scan Rate	4200 RPM	4200 RPM	Uniform Point Spacing
Target Pulse Rate	200 - 270 kHz	50 kHz	767 kHz
Pulse Length	2.5 ns	2.5 ns	3 ns
Laser Pulse Footprint Diameter	20 - 30 cm	190 - 285 cm	58.2 cm
Central Wavelength	1064 nm	515 nm	1064 nm
Pulse Mode	Continuous Multipulse	Continuous Multipulse	Multiple Times Around (MTA)
Beam Divergence	0.50 mrad	4.75 mrad	0.23 mrad
Swath Width	291 - 437 m	291 - 437 m	2836 m
Swath Overlap	70%	70%	55%
Intensity	16-bit	16-bit	16-bit

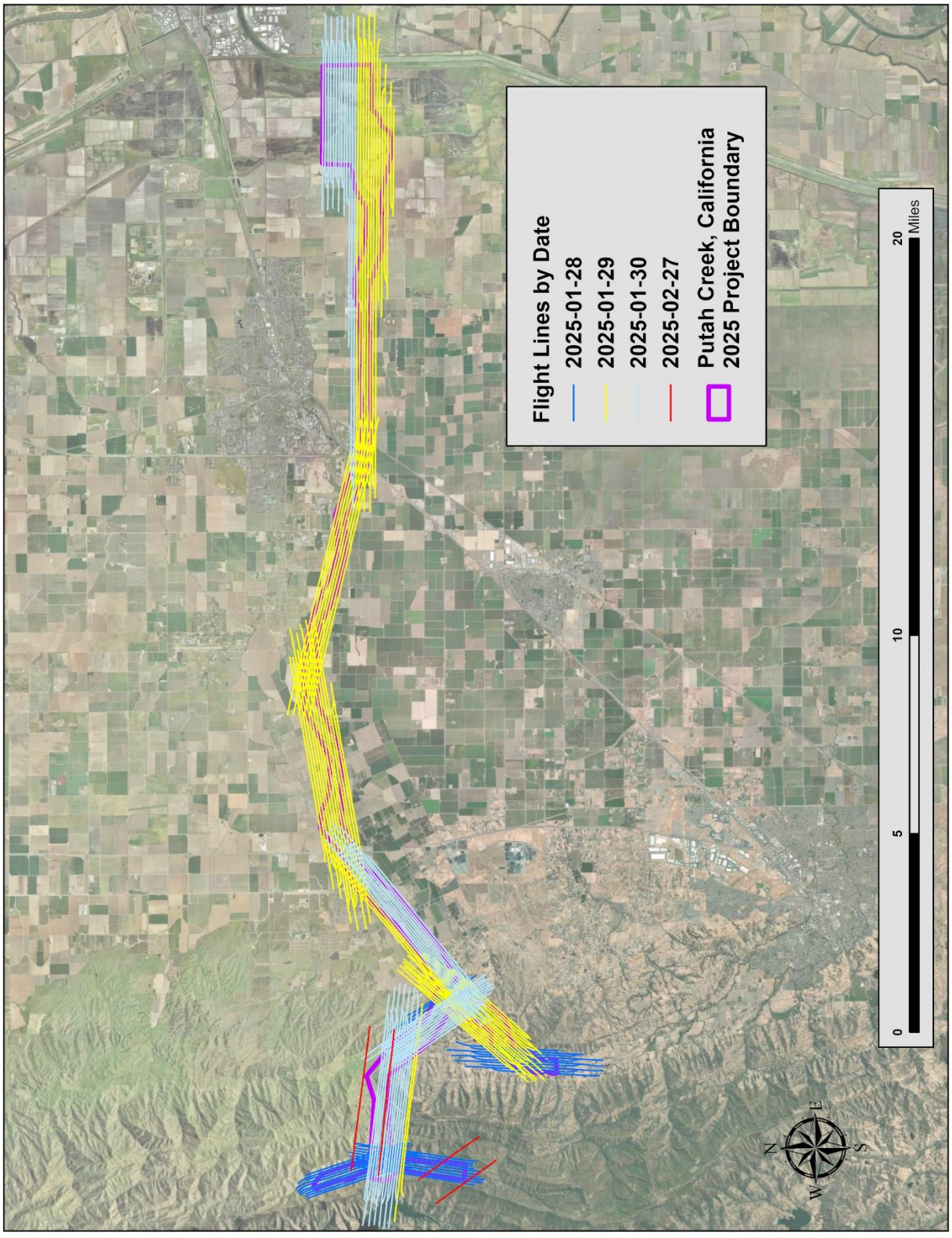

Figure 6: Flightlines map

Digital Imagery

Aerial imagery was co-acquired (with the lidar) using an integrated RCD30 digital camera (Table 7). The RCD30 is a medium format aerial mapping camera which collects imagery in four spectral bands (Red, Green, Blue, and Near-Infrared).

Table 7: Camera manufacturer's specifications for a RCD30

Parameter	RCD30 Specification
Focal Length	53 mm
Spectral Bands	Red, Green, Blue, Near-Infrared
Pixel Size	5.2 µm
Image Size	10,336 x 7,788 pixels
Frame Rate	GPS triggered
FOV	54° x 42°
Data Format	8bit TIFF

For the Putah Creek site, 3,588 images were collected in 106 flightlines with 60% along track overlap and 30% sidelap between frames. The acquisition flight parameters were designed to yield a native pixel resolution of ≤ 0.25 feet. Please note that imagery acquisition is not yet complete; the current collection covers 6,855 acres of the buffered boundary. A future acquisition will collect the remaining imagery (Figure 7). Orthophoto specifications particular to the Putah Creek project are in Table 8.

Table 8: Project-specific orthophoto specifications

Parameter	Digital Orthophotography Specification
Ground Sampling Distance (GSD)	≤ 0.25 ft pixel size
Along Track Overlap	≥60%
Cross Track Overlap	≥30%
Height Above Ground Level (AGL)	500 m
GPS PDOP	≤3.0
GPS Satellite Constellation	≥6

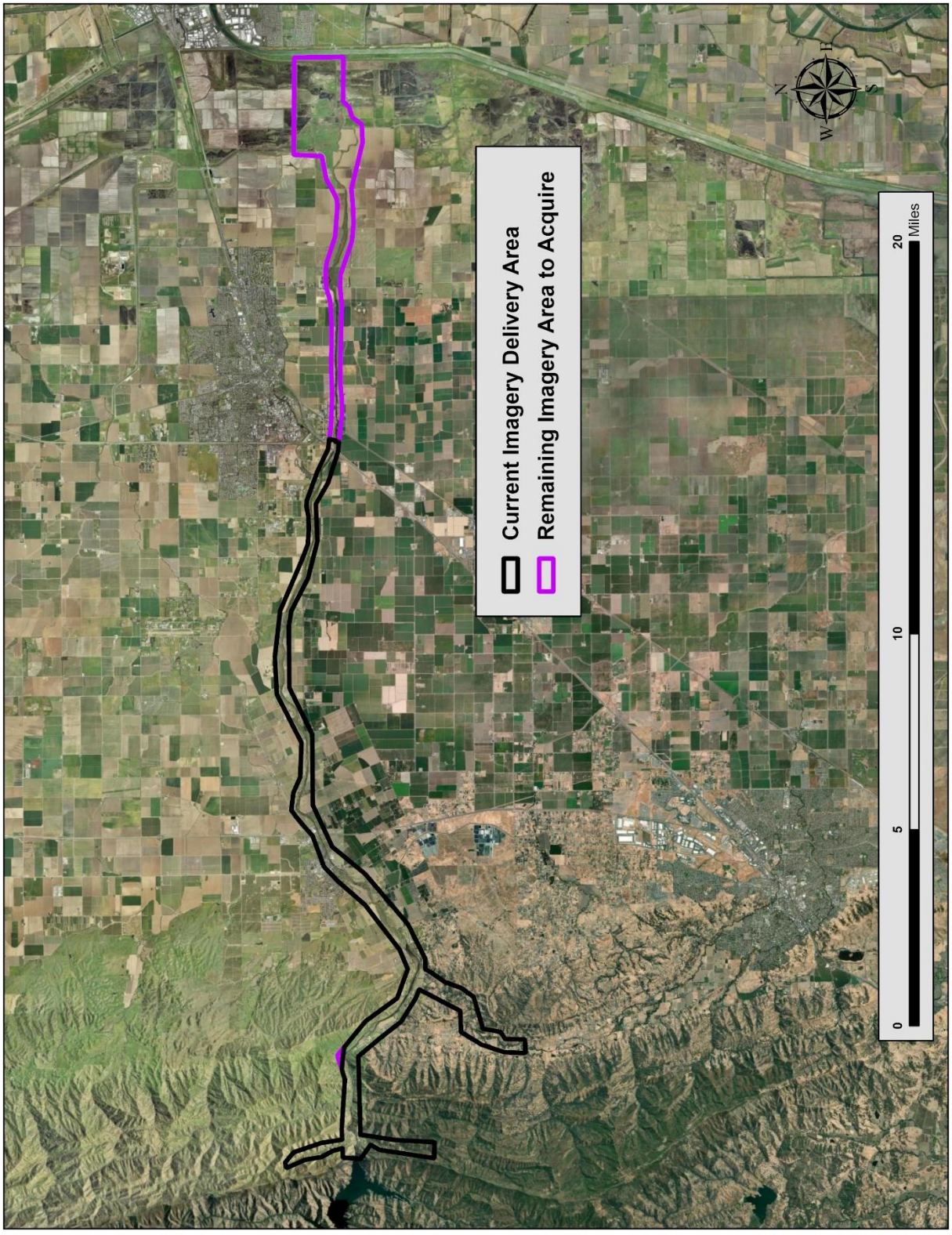

Figure 7: Current delivery and remaining imagery area

Ground Survey

Ground control surveys, including monumentation, aerial targets, and ground survey points (GSPs), were conducted to support the airborne acquisition. Ground control data were used to geospatially correct the aircraft positional coordinate data and to perform quality assurance checks on final lidar data, lidar derived products, and orthoimagery products.

NV5-established monument, PUTAH_01 survey photos; with survey equipment (above), and a close-up of nail with survey washer (right).

Base Stations

Base station locations were selected with consideration for satellite visibility, field crew safety, and optimal location for GSP coverage (Figure 9). NV5 utilized three permanent real-time network (RTN) base stations from the SmartNet and the California Surveying and Drafting Supply (CSDS) networks and established one new monument for the Putah Creek project (Table 9). The new monument was set using a 6" mag hub nail with an orange survey washer. NV5's professional land surveyor, Evon Silvia (CAPLS#9401), oversaw and certified the ground survey.

Table 9: Base station positions for the Putah Creek acquisition. Coordinates are on the NAD83(2011) datum, epoch 2010.00.

Monument ID	Latitude	Longitude	Ellipsoid (meters)	Owner	Type
CADN	38° 28' 20.45576"	-121° 49' 14.88129"	-3.219	SMARTNET	RTN
PUTAH_01	38° 30' 43.31549"	-122° 05' 49.48032"	37.340	NV5	MagNail
VV1J	38° 21' 15.91007"	-121° 59' 24.49627"	33.591	CSDS	RTN
WD1J	38° 40' 29.91466"	-121° 46' 03.07613"	0.511	CSDS	RTN

NV5 utilized static Global Navigation Satellite System (GNSS) data collected at 1 Hz recording frequency for each base station. During post-processing, the static GNSS data was triangulated with nearby Continuously Operating Reference Stations (CORS) using the Online Positioning User Service (OPUS[1]) for precise positioning. Multiple independent sessions over the same monument were processed to confirm antenna height measurements and to refine position accuracy.

[1] OPUS is a free service provided by the National Geodetic Survey to process corrected monument positions: OPUS website

Monuments were established according to the national standard for geodetic control networks, as specified in the Federal Geographic Data Committee (FGDC) Geospatial Positioning Accuracy Standards for geodetic networks.[2] This standard provides guidelines for classification of monument quality at the 95% confidence interval as a basis for comparing the quality of one control network to another. The monument rating for this project is shown in Table 10.

Table 10: Federal Geographic Data Committee monument rating for network accuracy

Direction	Rating
1.96 * St Dev $_{NE}$:	0.020 m
1.96 * St Dev $_{z}$:	0.020 m

For the Putah Creek Lidar project, the monument coordinates contributed no more than 2.8 cm of positional error to the geolocation of the final ground survey points and lidar, with 95% confidence.

Ground Survey Points (GSPs)

Ground survey points were collected using real time kinematic (RTK) survey techniques. For RTK surveys, a roving receiver receives corrections from a nearby base station or Real-Time Network (RTN) via radio or cellular network, enabling rapid collection of points with relative errors less than 1.5 cm horizontal and 2.0 cm vertical. RTK surveys record data while stationary for at least five seconds, calculating the position using at least three one-second epochs. All GSP measurements were made during periods with a Position Dilution of Precision (PDOP) of ≤3.0 with at least six satellites in view of the stationery and roving receivers. See Table 11 for NV5 ground survey equipment information.

GSPs were collected in areas where good satellite visibility was achieved on paved roads and other hard surfaces such as gravel or packed dirt roads. GSP measurements were not taken on highly reflective surfaces such as center line stripes or lane markings on roads due to the increased noise seen in the laser returns over these surfaces. GSPs were collected within as many flightlines as possible; however, the distribution of GSPs depended on ground access constraints and monument locations and may not be equably distributed throughout the study area (Figure 9).

Table 11: NV5 ground survey equipment identification.

Receiver Model	Antenna	OPUS Antenna ID	Use
Trimble R750	Zephyr Model 3 GNSS	TRM115000.10	Static
Trimble R12	Integrated Antenna	TRMR12	Rover

[2] Federal Geographic Data Committee, ASPRS POSITIONAL ACCURACY STANDARDS FOR DIGITAL GEOSPATIAL DATA Edition 2, Version 2, 2024

Aerial Targets

Air target points (ATPs) were collected throughout the project area prior to imagery acquisition to refine the exterior orientation parameters of the camera and to conduct an accuracy assessment of the final orthophoto product. ATPs are typically collected over hard surface ground features or temporary vinyl chevrons. Hard surface points consist of high contrast road markings such as stop bars and turn arrows and cement corners (Figure 8). Each ATP was surveyed using RTK techniques and locations are represented on the map in Figure 9.

Figure 8: Examples of aerial targets collected for the Putah Creek project

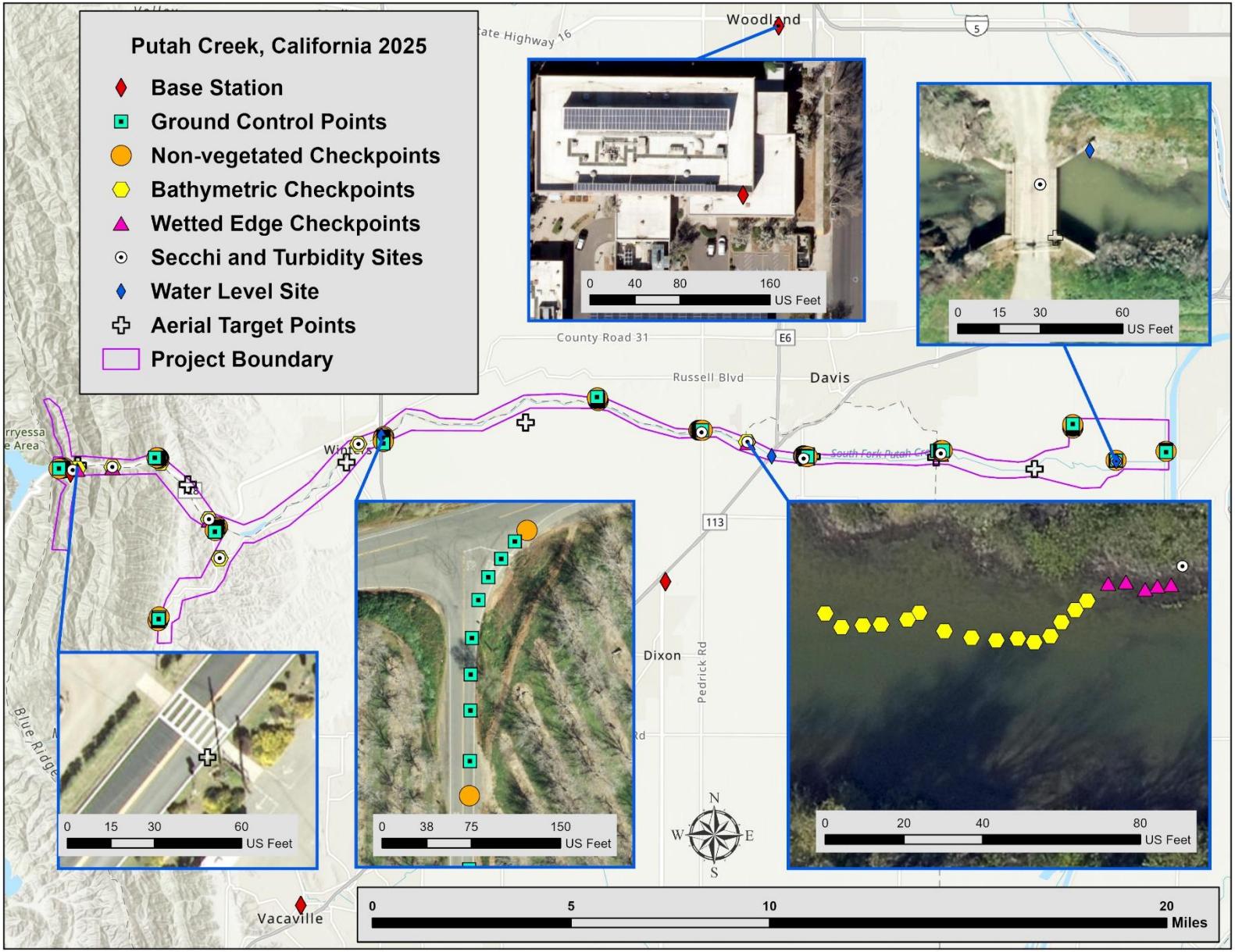

Figure 9: Ground survey location map

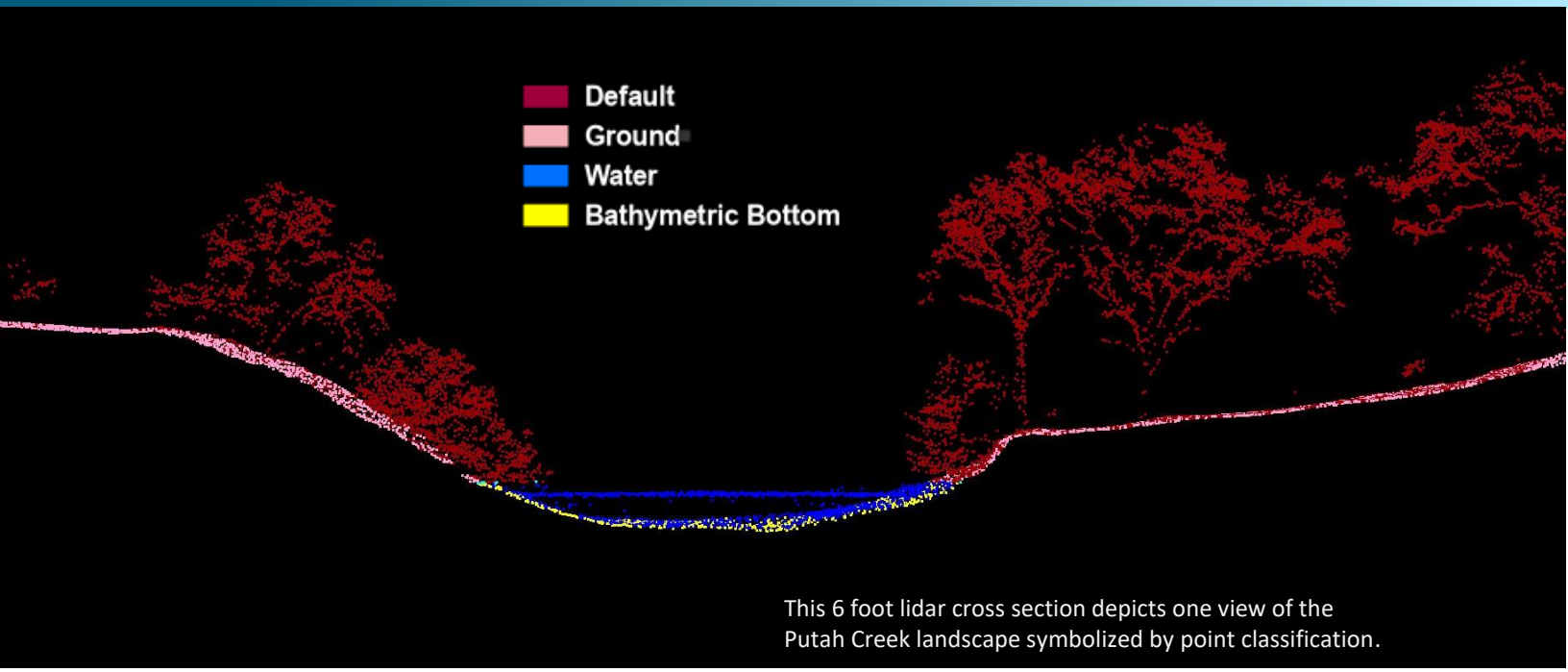

This 6 foot lidar cross section depicts one view of the Putah Creek landscape symbolized by point classification.

Topobathymetric Lidar Data

Upon completion of data acquisition, NV5 processing staff initiated a suite of automated and manual techniques to process the data into the requested deliverables. Processing tasks included GPS control computations, smoothed best estimate trajectory (SBET) calculations, kinematic corrections, calculation of laser point position, sensor and data calibration for optimal relative and absolute accuracy, and lidar point classification (Table 12).

Leica Lidar Survey Studio (LSS) software was used to facilitate bathymetric return processing. Once bathymetric points were differentiated, they were spatially corrected for refraction through the water column based on the angle of incidence of the laser. The resulting point cloud data was classified using both manual and automated techniques. Processing methodologies were tailored for the landscape. Brief descriptions of these tasks are shown in Table 13.

Bathymetric Refraction

Following final SBET creation for the Leica Chiroptera 5X, NV5 used LSS to calculate laser point positioning by associating SBET positions to each laser point return time, scan angle, and intensity. LSS was used to derive a synthetic water surface to create a water surface model. Light travels at different speeds in air versus water and its direction of travel or angle is changed or refracted when entering the water column. The refraction tool corrects for this difference by adjusting the depth (distance traveled) and horizontal positioning (change of angle/direction) of the lidar data. LSS then outputs the lidar point cloud as classified LAS 1.4 files.

Table 12: ASPRS LAS classification standards applied to the Putah Creek dataset.

Classification Number	Classification Name	Classification Description
1	Default	Laser returns that are not included in the ground class, composed of vegetation and anthropogenic features.
2	Ground	Laser returns that are determined to be ground using automated and manual cleaning algorithms.
40	Bathymetric Bottom	Refracted green laser returns that fall within the water's edge breakline which characterize the submerged topography.
41	Water Surface	Green laser returns that are determined to be water surface points using automated and manual cleaning algorithms.
42	Synthetic Water Surface	Synthetically generated water surface.
45	Water Column	Refracted green sensor returns that are determined to be water (between the water surface and bathymetric bottom) using automated and manual cleaning algorithms.

Table 13: Lidar processing workflow

Lidar Processing Step	Software Used
Resolve kinematic corrections for aircraft position data using kinematic aircraft GPS and static ground GPS data. Develop a smoothed best estimate of trajectory (SBET) file that blends post-processed aircraft position with sensor head position and attitude recorded throughout the survey.	Inertial Explorer v.9.0.2 MoveOut (NV5 proprietary)
Calculate laser point position by associating SBET position to each laser point return time, scan angle, intensity, etc. Create raw laser point cloud data for the entire survey in *.las (ASPRS v. 1.4) format. Convert data to orthometric elevations by applying a geoid correction.	Lidar Survey Studio v.3.4.3 Las Projector v.1.5.9 RiUnite v.1.0.9
Import raw laser points into manageable blocks to perform manual relative accuracy calibration and filter erroneous points. Classify ground points for individual flight lines.	TerraScan v.19.005
Using ground classified points per each flight line, test the relative accuracy. Perform automated line-to-line calibrations for system attitude parameters (pitch, roll, heading), mirror flex (scale), and GPS/IMU drift. Calculate calibrations on ground classified points from paired flight lines and apply results to all points in a flight line. Use every flight line for relative accuracy calibration.	StripAlign v.2.24
Apply refraction correction to all subsurface returns.	Las Monkey v.2.6.9 (NV5 proprietary)
Classify resulting data to ground and other client designated ASPRS classifications (Table 12). Assess statistical absolute accuracy via direct comparisons of ground classified points to ground control survey data.	TerraScan v.19.005 TerraModeler v.19.003
Generate bare earth models as triangulated surfaces. Generate highest hit models as a surface expression of all classified points. Export all surface models as Cloud-Optimized GeoTIFFs, (.tif) format at a 1.5 foot pixel resolution.	Las Product Creator v.4.0 (NV5 proprietary)
Export intensity images as cloud optimized GeoTIFFs at a 1.5 foot pixel resolution.	Las Product Creator v.4.0 (NV5 proprietary)

Lidar Derived Products

Because hydrographic laser scanners penetrate the water surface to map submerged topography, this affects how the data should be processed and presented in derived products from the lidar point cloud. The following section discusses certain derived products that vary from the traditional (NIR) specification and delivery format.

Topobathymetric DEMs

Bathymetric bottom returns can be limited by depth, water clarity, and bottom surface reflectivity. Water clarity and turbidity affect the depth penetration capability of the green wavelength laser with returning laser energy diminishing by scattering throughout the water column. Additionally, the bottom surface must be reflective enough to return remaining laser energy back to the sensor at a detectable level. Although the predicted depth penetration range of the Chiroptera CH5X sensor is 1.5x Secchi depths on brightly reflective surfaces, it is not unexpected to have no bathymetric bottom returns in turbid or non-reflective areas.

As a result, creating digital elevation models (DEMs) presents a challenge with respect to interpolation of areas with no returns. Traditional DEMs are “unclipped”, meaning areas lacking ground returns are interpolated from neighboring ground returns (or breaklines in the case of hydro-flattening), with the assumption that the interpolation is close to reality. In bathymetric modeling, these assumptions are prone to error because a lack of bathymetric returns can indicate a change in elevation that the laser can no longer map due to increased depths. The resulting void areas may suggest greater depths, rather than similar elevations from neighboring bathymetric bottom returns. Therefore, NV5 created a water polygon with bathymetric coverage to delineate areas with successfully mapped bathymetry. This shapefile was used to control the extent of the delivered clipped topobathymetric model to avoid false triangulation (interpolation from TIN’ing) across areas in the water without bathymetric bottom returns.

Feature Extraction

Residual Pools

A residual pool refers to the depth and volume of water remaining in a pool after the flow has stopped draining over the downstream riffle crest. NV5 identified residual pools in Putah Creek using the topobathymetric lidar models. Residual pool depth, area, and volume were then computed by filling internal drainage areas or sinks within the floodplain and created a set of polygon shapes. Elevation minimums and maximums were also calculated and attributed. This data set represents pool conditions under base flows.

Relative Elevation Models

Relative Elevation Models (REMs) provide useful information for analyses related to floodplain mapping and fluvial morphology. REMs are especially useful in visualizing fluvial features like oxbow lakes, paleo-channels, cutoff meanders, and terraces. REMs display the relative height above the local river water surface by detrending the model baseline elevation to follow the stream surface elevation.

Before the REM can be generated, the water's edge breaklines are delineated and a stream centerline of the main channel is produced. This stream centerline ensures that the elevations are pulled from the channel migration zones in the main channel. A transect-based method was then used to produce the REMs. Transects used in development of the REM were made to not cross each other and to be as close to perpendicular as possible to the centerline (Figure 10). The lowest water surface elevations along the main channel were extracted along each transect and used to produce a triangulated irregular network (TIN). This raster was then subtracted from the water surface model to produce the REM. The TIN is used to create a river slope trend surface, which is then subtracted from the original DEM. Values equaling or exceeding 15 feet were reclassed with a value of 15 feet within each respective REM to not misrepresent high elevation slopes, but to support graphic visualization.

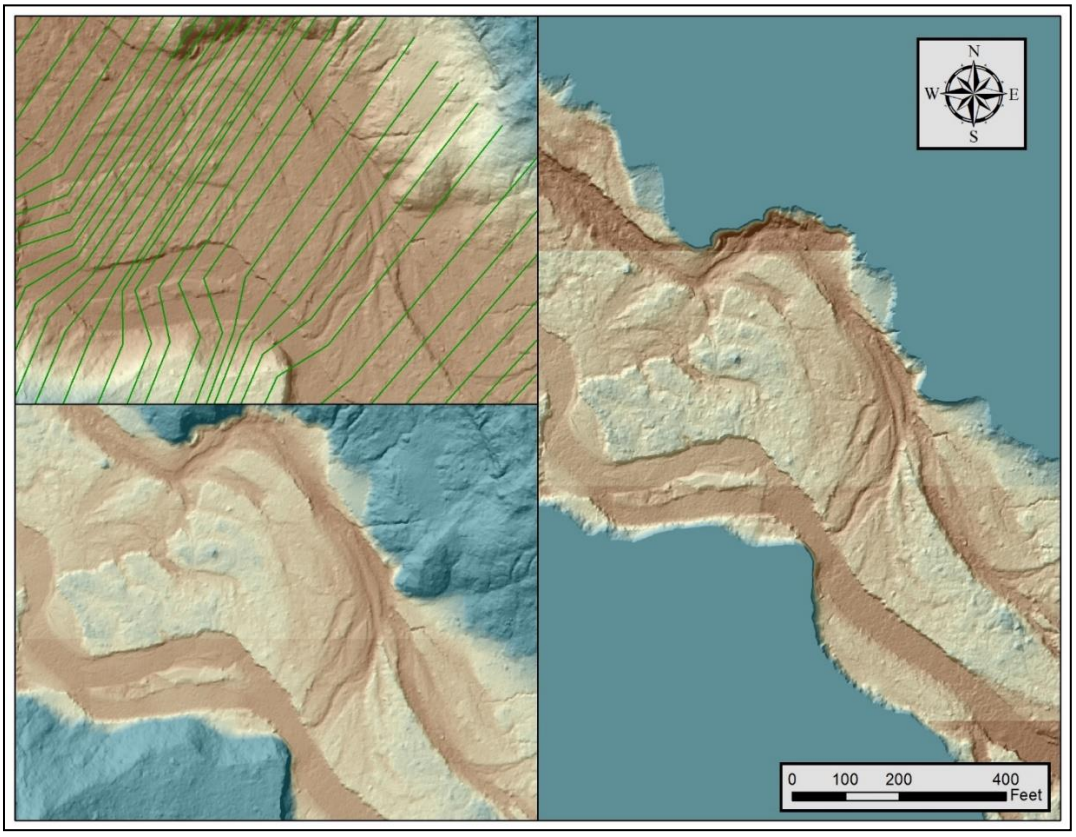

Figure 10: A graphic of relative elevation models (REMs).The image in the upper left shows the transects, the bottom left shows the REM overlaid on top of the bare earth hillshade, while the image on the right shows the REM overlaid on the REM hillshade.

Digital Imagery

As with the lidar, the collected digital photographs went through multiple processing steps to create final orthophoto products. Initially, mission wide color balancing was performed to improve image contrast and tonality, then output as 8bit (4band), geometrically corrected tiff files. Photo position and orientation were then calculated by linking the time of image capture to the smoothed best estimate of trajectory (SBET) file created during lidar post-processing. Within Inpho Match AT, an automated aerial triangulation was performed to refine exterior orientation parameters of the camera and adjust the photo block to ground control.

Adjusted images were orthorectified using the lidar-derived ground model to remove displacement effects from topographic relief inherent in the imagery. The resulting orthophotos were mosaicked within Inpho OrthoVista, blending seams and applying automated project color-balancing. Aerial imagery was collected as a supplemental product to lidar. As such, flight planning prioritized water conditions for bathymetric lidar collection which may not always be optimal for imagery. Imagery processing included global color-balancing and automated seamline generation; however cutlines may exist through buildings or other manmade features. The processing workflow for orthophotos is summarized in Table 14.

Table 14: Orthophoto processing workflow

Orthophoto Processing Step	Software Used
Resolve GPS kinematic corrections for the aircraft position data using kinematic aircraft GPS (collected at 2 Hz) and PPP data.	Inertial Explorer v9
Develop a smooth best estimate trajectory (SBET) file that blends post-processed aircraft position with attitude data. Sensor heading, position, and attitude are calculated throughout the survey.	Inertial Explorer v9
Resolve exterior orientation (EO) for each image event with omega, phi, and kappa.	HxMap v4.5
Convert raw imagery data into geometrically corrected TIFF images.	HxMap v4.5
Apply EO to photos, and perform aerial triangulation using automatically generated tie points and ground control data.	Inpho Match AT v14.1
Import DEM and orthorectify image frames	Inpho OrthoMaster v14.1
Mosaic orthorectified imagery blending automated and manually drawn seams between photos and applying global color balancing to the project.	Inpho OrthoVista/SeamEditor v14.1

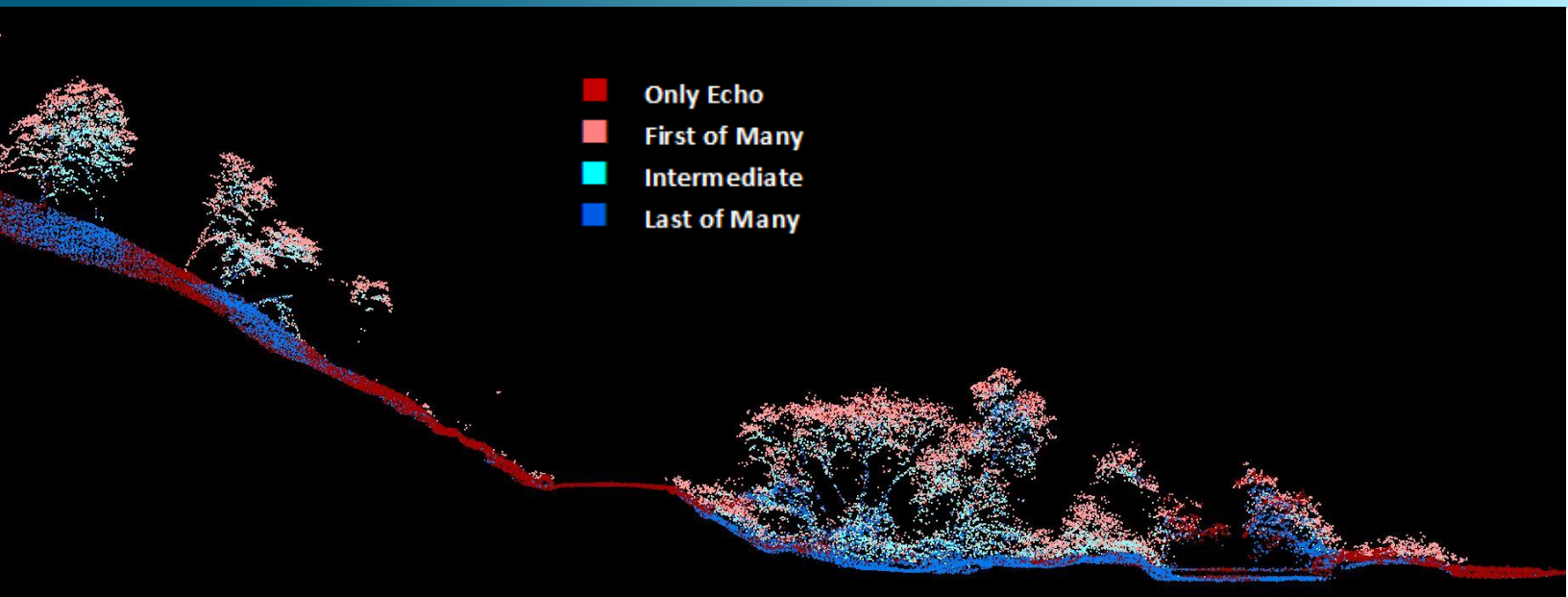

This 13 foot lidar cross section shows a view of vegetation and bare ground in the Putah Creek project, symbolized by point laser echo.

Bathymetric Lidar

An underlying principle for collecting hydrographic lidar data is to survey near-shore areas that can be difficult to collect with other methods, such as multi-beam sonar, particularly over large areas. The capability and effectiveness of the bathymetric lidar is impacted by several parameters including depth penetrations below the water surface, bathymetric return density, and spatial accuracy.

Mapped Bathymetry and Depth Penetration

Under optimal conditions, the specified depth penetration range of the CH5X is about 1.5 Secchi depths. To assist in evaluating performance results of the sensor, a polygon layer was created to delineate areas where bathymetry was successfully mapped. This coverage shapefile was used to control the extent of the delivered clipped topo-bathymetric model and to avoid false triangulation across areas in the water with no returns. Insufficiently mapped areas were identified by triangulating bathymetric bottom points with an edge length maximum of 15.2 feet. This ensured all areas of no returns (>96.88 ft^2), were identified as data voids. Overall NV5 successfully mapped 45.85% of the bathymetric areas in the Putah Creek AOI. Of the areas successfully mapped, 66.23% had a calculated depth of 0 - 2 feet, 23.44% had a depth of 2.01 - 4 feet, 6.71% had a depth of 4.01 - 6 feet, 2.24% had a depth of 6.01 - 8 feet, 0.76% had a depth of 8.01 - 10 feet, and the remaining 0.62% had a calculated depth greater than 10 feet (Figure 10). The maximum recorded depth for the Putah Creek topobathymetric dataset was 21.90 feet.

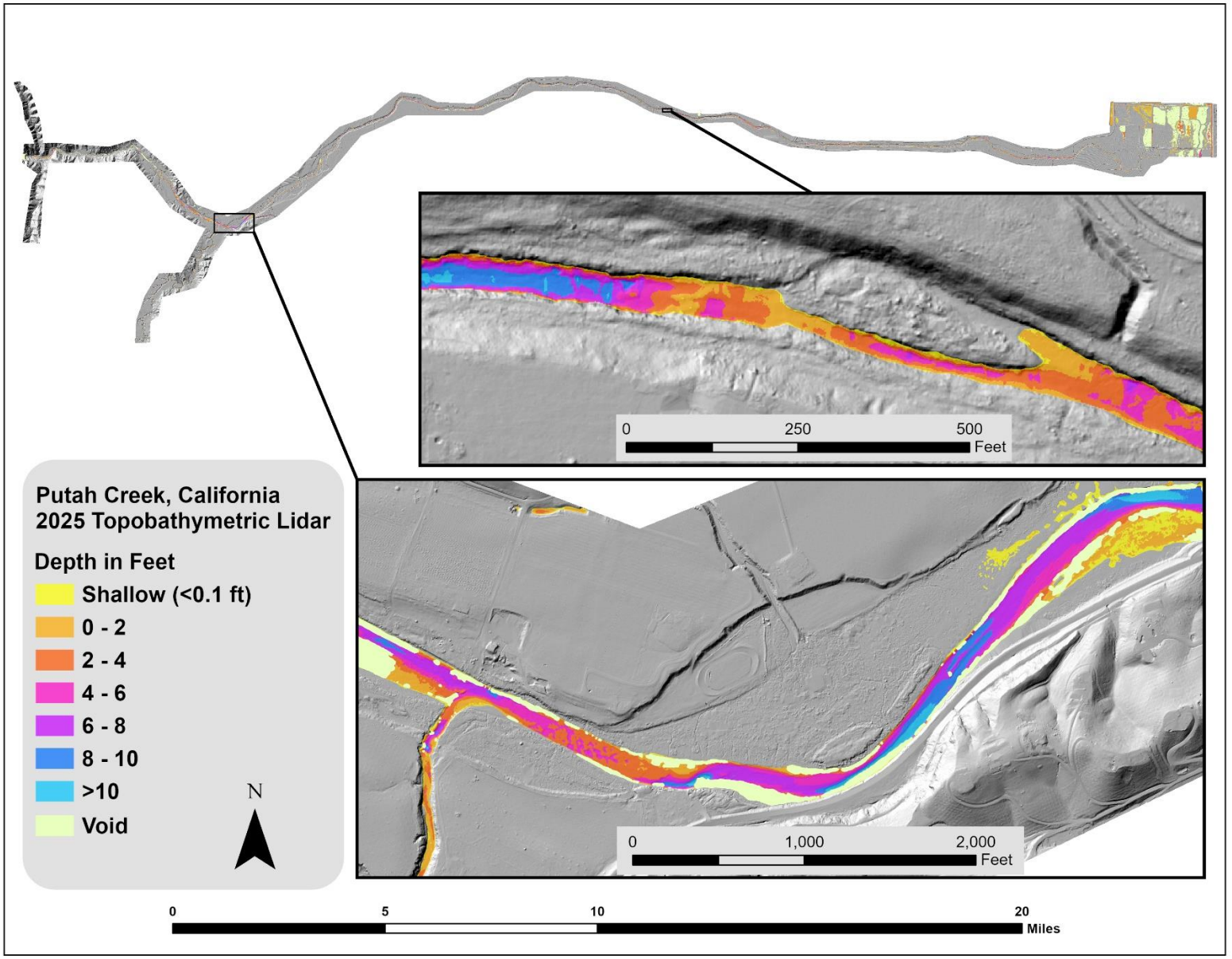

Figure 10: Depth model for Putah Creek

Lidar Point Density

First Return Point Density

The acquisition parameters were designed to acquire an average first-return density of 8 points/m^2 (0.74 points/ft^2). First return density describes the density of pulses emitted from the laser that return at least one echo to the system. Multiple returns from a single pulse were not considered in first return density analysis. Some types of surfaces (e.g., breaks in terrain, water, and steep slopes) may have returned fewer pulses than originally emitted by the laser.

First returns typically reflect off the highest feature on the landscape within the footprint of the pulse. In forested or urban areas the highest feature could be a tree, building, or power line, while in areas of unobstructed ground, the first return will be the only echo and represents the bare earth surface. The average first-return density of the Putah Creek lidar project was 32.04 points/m^2 (2.98 points/ft^2) (Table 15). The statistical and spatial distributions of all first return densities per 100 x 100 meter cell are portrayed in Figure 11 and Figure 13.

Bathymetric and Ground Classified Point Densities

The density of ground classified lidar returns and bathymetric bottom returns were also analyzed for this project. Terrain character, land cover, and ground surface reflectivity all influenced the density of ground surface returns. In vegetated areas, fewer pulses may have penetrated the canopy, resulting in lower ground density. Similarly, the density of bathymetric bottom returns was influenced by turbidity, depth, and bottom surface reflectivity. In turbid areas, fewer pulses may have penetrated the water surface, resulting in lower bathymetric density.

The ground and bathymetric bottom classified density of lidar data for the Putah Creek project was 16.16 points/m^2 (1.50 points/ft^2) (Table 15). The statistical and spatial distributions per 100 x 100 meter cell of the ground and bathymetric bottom classified return densities are portrayed in Figure 12 and Figure 14.

Additionally, for the Putah Creek project, density values of only bathymetric bottom returns were calculated for areas containing at least one bathymetric bottom return. Areas lacking bathymetric returns (voids) were not considered in calculating an average density value. Within the successfully mapped area, a bathymetric bottom return density of 6.93 points/m^2 (0.64 points/ft^2) was achieved.

Table 15: Average point density.

Density Type	Point Density
First Returns	2.98 points/ft² 32.04 points/m²
Ground and Bathymetric Bottom Classified Returns	1.50 points/ft² 16.16 points/m²
Bathymetric Bottom Classified Returns	0.64 points/ft² 6.93 points/m²

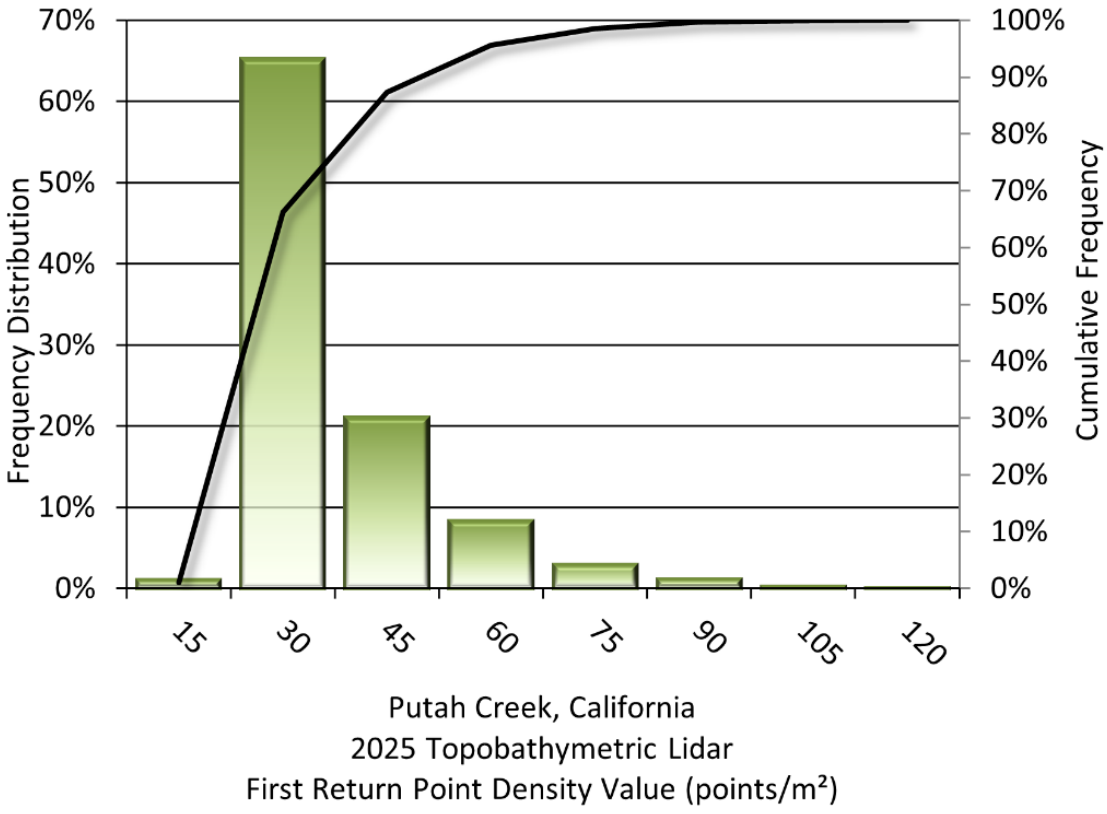

Figure 11: Frequency distribution of first return density per 100 x 100 meter cell.

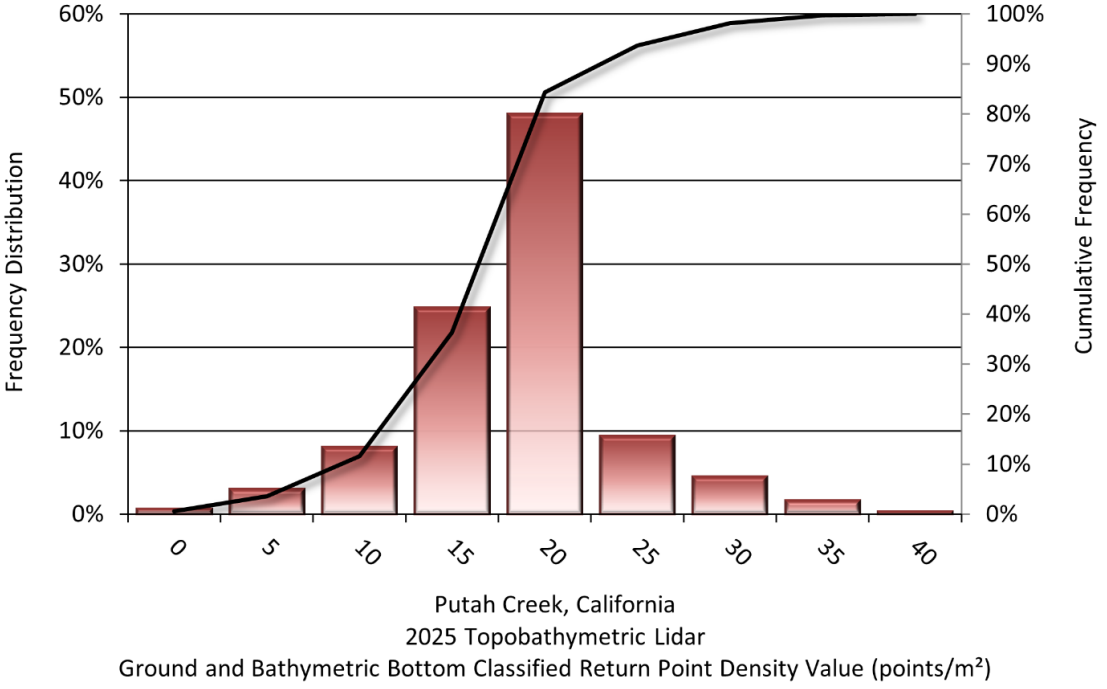

Figure 12: Frequency distribution of ground and bathymetric bottom classified return density per 100 x 100 meter cell.

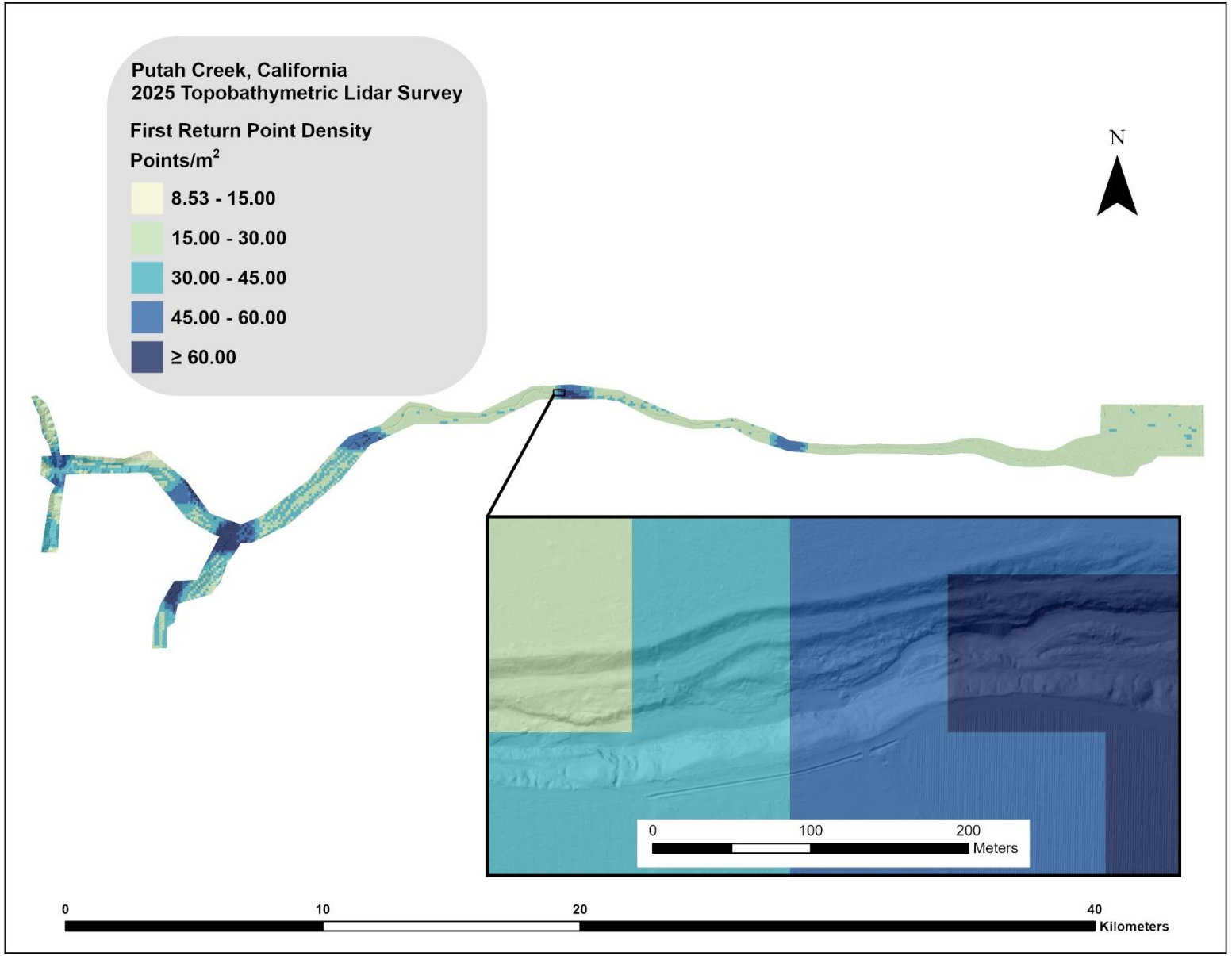

Figure 13: First return density map for the Putah Creek site (100 x 100 meter cells).

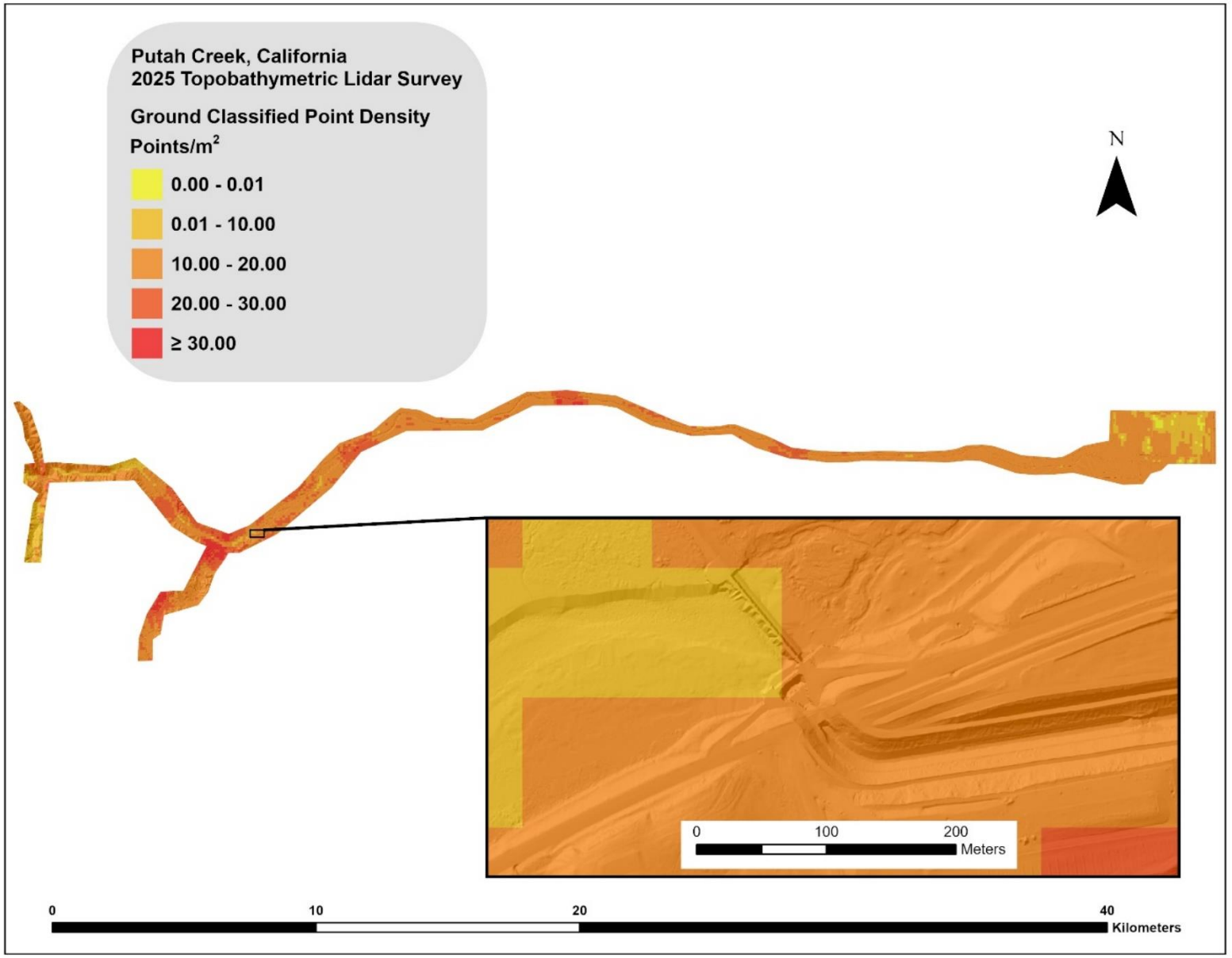

Figure 14: Ground classified density map for the Putah Creek site (100 x 100 meter cells).

Lidar Accuracy Assessments

The accuracy of the lidar data collection can be described in terms of absolute accuracy (the consistency of the data with external data sources) and relative accuracy (the consistency of the dataset with itself). See Appendix A for further information on sources of error and operational measures used to improve relative accuracy.

Lidar Non-Vegetated Vertical Accuracy

Absolute accuracy was assessed using Non-vegetated Vertical Accuracy (NVA) reporting designed to meet guidelines presented in the FGDC National Standard for Spatial Data Accuracy.[3] NVA compares known ground check point data that were withheld from the calibration and post-processing of the lidar point cloud to the triangulated surface generated by the classified lidar point cloud as well as the derived gridded bare earth DEM. NVA is a measure of the accuracy of lidar point data in open areas where the lidar system has a high probability of measuring the ground surface and is evaluated at the 95% confidence interval (1.96 * RMSE), as shown in Table 16.

The mean and standard deviation (sigma σ) of divergence of the ground surface model from ground check point coordinates are also considered during accuracy assessment. These statistics assume the error for x, y, and z is normally distributed, and therefore the skew and kurtosis of distributions are also considered when evaluating error statistics. For the Putah Creek survey, 35 ground checkpoints were withheld from the calibration and post-processing of the lidar point cloud, with resulting non-vegetated vertical accuracy of 0.053 meters (0.173 feet) as compared to the classified LAS, and 0.053 meters (0.174 feet) against the bare earth DEM, with 95% confidence (Table 16, Figure 15, Figure 16).

NV5 also assessed absolute accuracy using 280 ground control points. Although these points were used in the calibration and post-processing of the lidar point cloud, they still provide a good indication of the overall accuracy of the lidar dataset, and therefore have been provided in Table 16 and Figure 17.

[3] Federal Geographic Data Committee, ASPRS POSITIONAL ACCURACY STANDARDS FOR DIGITAL GEOSPATIAL DATA Edition 2, Version 2, 2024. https://asprsorg.sharepoint.com/sites/PublicAccess/Shared%20Documents/Forms/AllItems.aspx?id=%2Fsites%2FPublicAccess%2FShared%20Documents%2FPublic%5FDocuments%2FStandards%2F2024%5FASPRS%5FPositional%5FAccuracy%5FStandards%5FEdition2%5FVersion2%2E0%2Epdf&parent=%2Fsites%2FPublicAccess%2FShared%20Documents%2FPublic%5FDocuments%2FStandards&p=true&ga=1.

Table 16: Absolute accuracy results.

Parameter	NVA, as compared to Classified LAS	NVA, as compared to Bare Earth DEM	Ground Control Points
Sample	35 points	35 points	280 points
95% Confidence (1.96*RMSE)	0.173 ft 0.053 m	0.174 ft 0.053 m	0.151 ft 0.046 m
Average	-0.017 ft -0.005 m	-0.016 ft -0.005 m	-0.008 ft -0.003 m
Median	0.003 ft 0.001 m	0.003 ft 0.001 m	0.010 ft 0.003 m
RMSE	0.088 ft 0.027 m	0.089 ft 0.027 m	0.077 ft 0.023 m
Standard Deviation (1σ)	0.088 ft 0.027 m	0.089 ft 0.027 m	0.077 ft 0.023 m

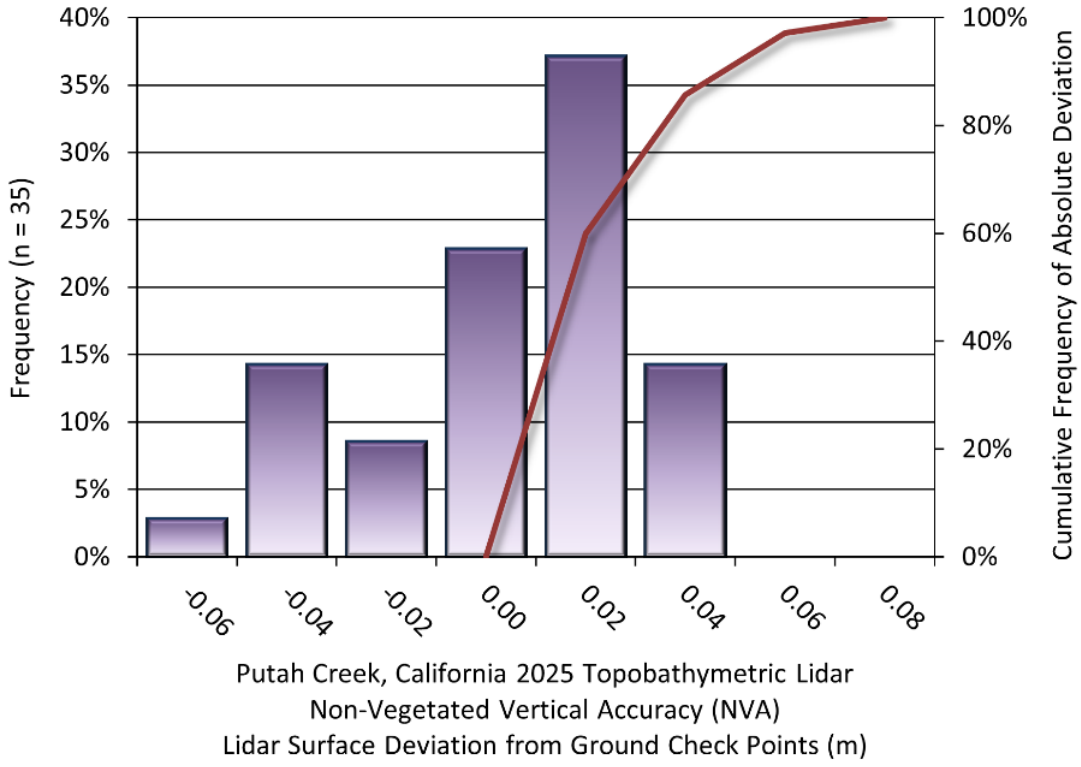

Figure 15: Frequency histogram for classified LAS deviation from ground check point values.

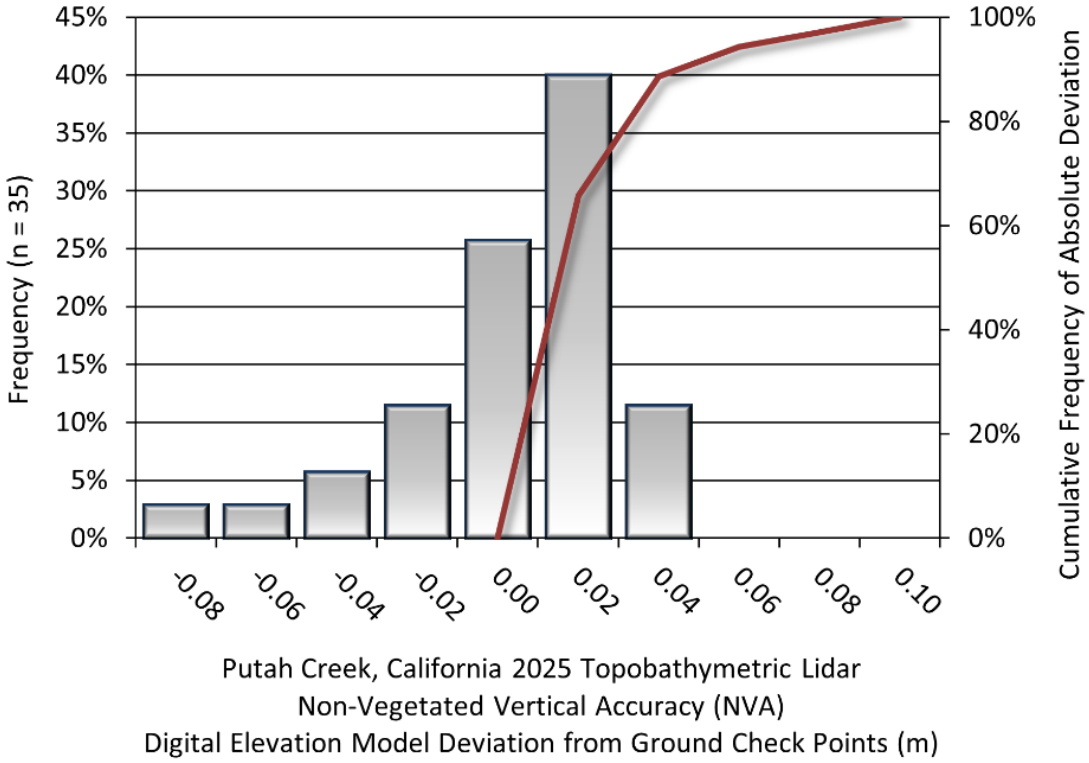

Figure 16: Frequency histogram for lidar bare earth DEM deviation from ground checkpoint values.

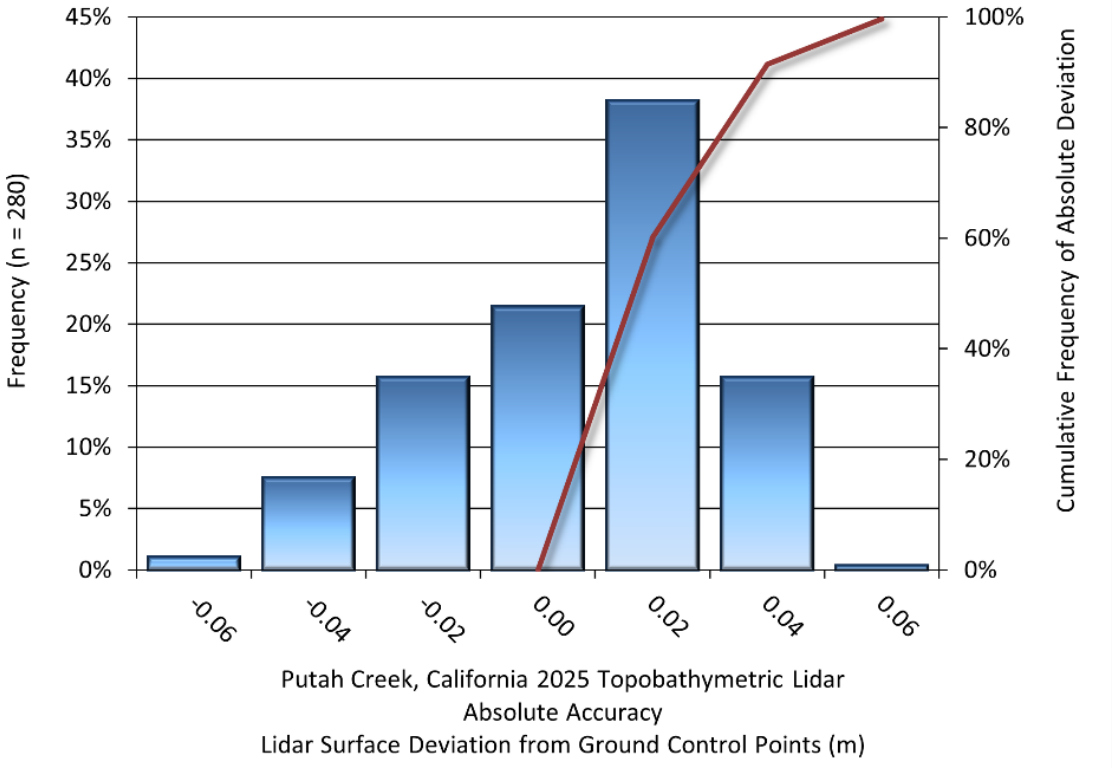

Figure 17: Frequency histogram for lidar surface deviation ground control point values.

Lidar Bathymetric Vertical Accuracies

Bathymetric (submerged or along the water's edge) checkpoints were also collected in order to assess the submerged surface vertical accuracy. Assessment of 115 submerged bathymetric checkpoints resulted in a vertical accuracy of 0.127 meters (0.415 feet), while assessment of 28 wetted edge checkpoints resulted in a vertical accuracy of 0.163 meters (0.535 feet) evaluated at 95% confidence interval (Table 17, Figure 18 and Figure 19).

Table 17: Bathymetric vertical accuracy.

Parameter	Submerged Bathymetric Checkpoints	Wetted Edge Bathymetric Checkpoints
Sample	115 points	28 points
95th Percentile	0.415 ft 0.127 m	0.535 ft 0.163 m
Average Dz	-0.046 ft -0.014 m	-0.106 ft -0.032 m
Median	-0.059 ft -0.018 m	-0.048 ft -0.015 m
RMSE	0.212 ft 0.065 m	0.273 ft 0.083 m
Standard Deviation (1σ)	0.208 ft 0.063 m	0.257 ft 0.078 m

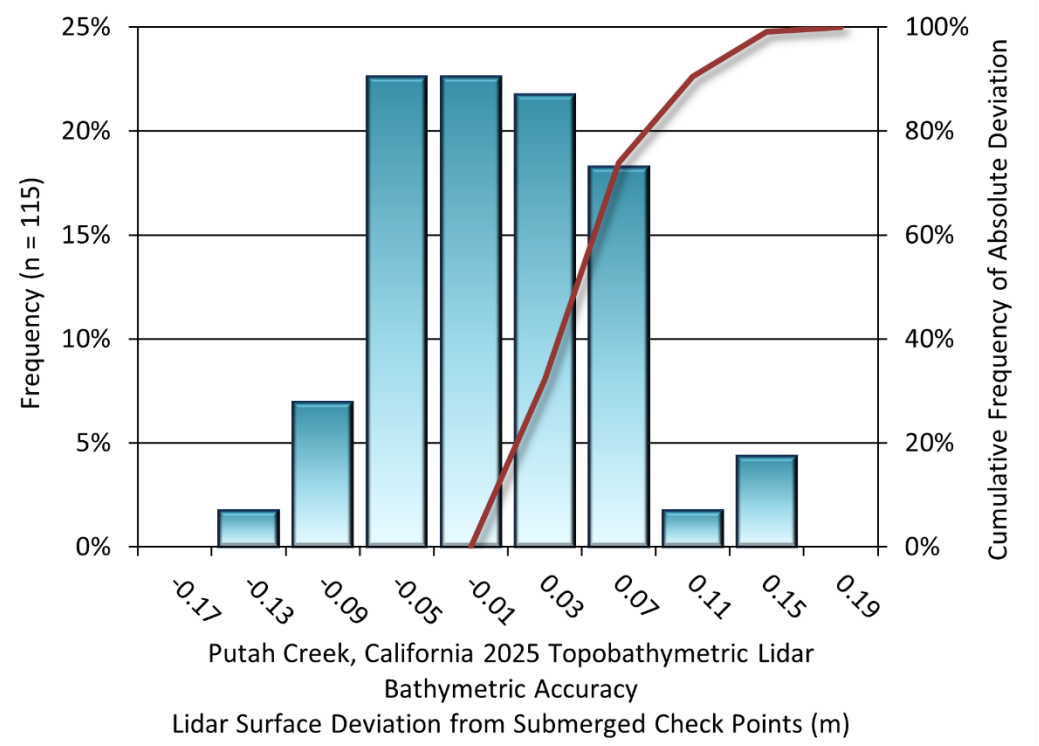

Figure 18: Frequency histogram for lidar surface deviation from submerged check point values.

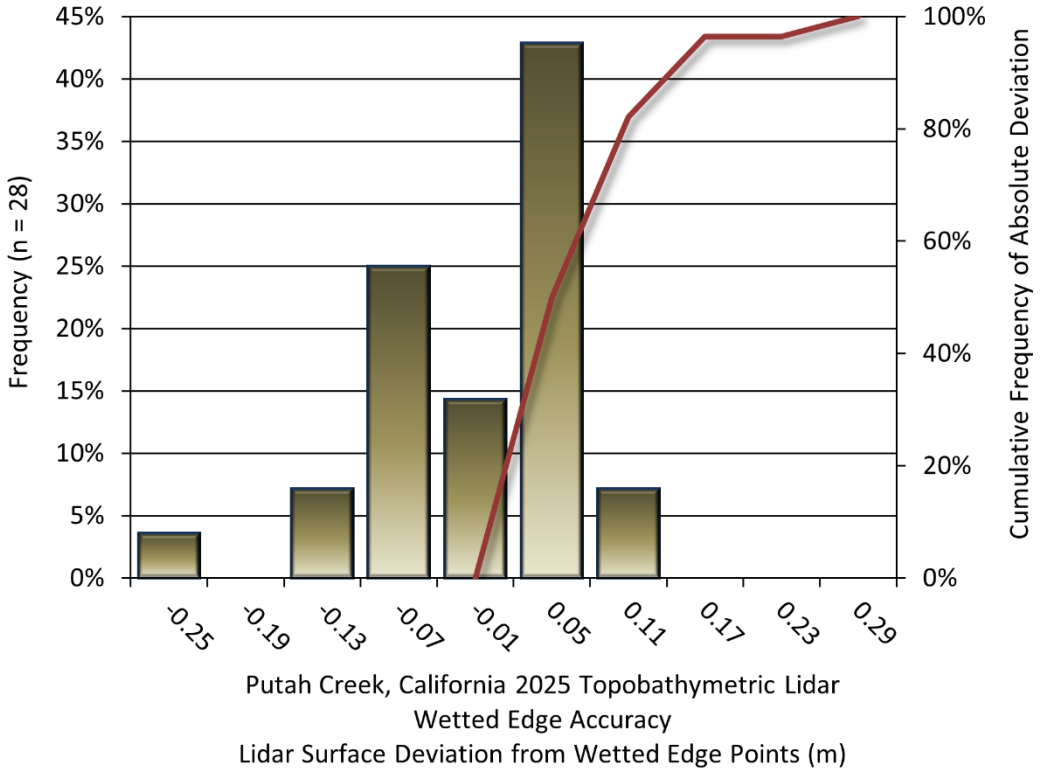

Figure 19: Frequency histogram for lidar surface deviation from wetted edge check point values.

Lidar Relative Vertical Accuracy

Relative vertical accuracy refers to the internal consistency of the data set as a whole: the ability to place an object in the same location given multiple flight lines, GPS conditions, and aircraft attitudes. When the lidar system is well calibrated, the swath-to-swath vertical divergence is low (<0.10 meters). The relative vertical accuracy was computed by comparing the ground surface model of each individual flight line with its neighbors in overlapping regions. The average (mean) line to line relative vertical accuracy for the Putah Creek Lidar project was 0.020 meters (0.065 feet) (Table 18, Figure 20).

Table 18: Relative accuracy results.

Parameter	Relative Accuracy
Sample	276 flight line surfaces
Average	0.065 ft 0.020 m
Median	0.111 ft 0.034 m
RMSE	0.135 ft 0.041 m
Standard Deviation (1σ)	0.069 ft 0.021 m
1.96σ	0.136 ft 0.041 m

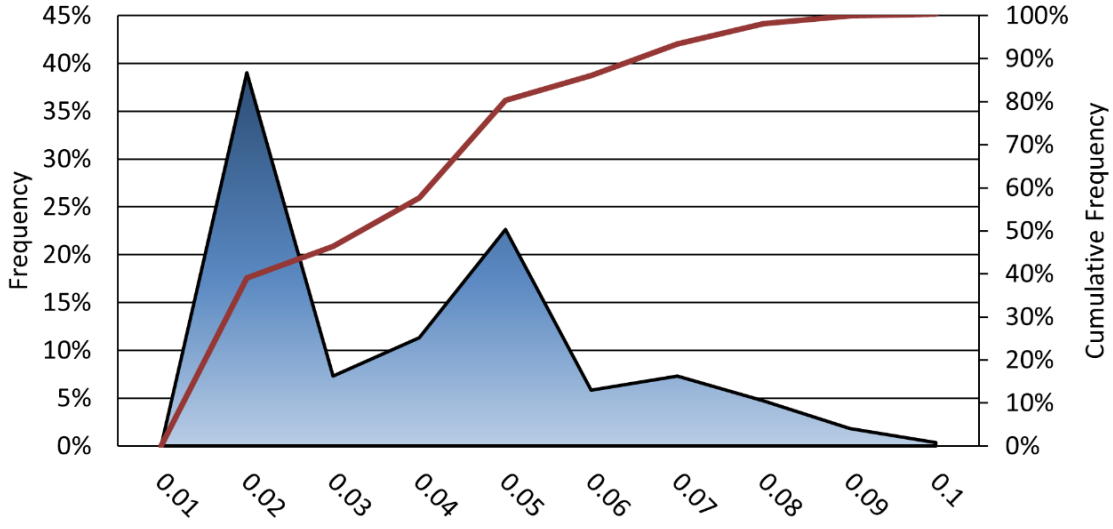

Figure 20: Frequency plot for relative vertical accuracy between flight lines.

Lidar Horizontal Accuracy

Lidar horizontal accuracy is a function of Global Navigation Satellite System (GNSS) derived positional error, flying altitude, and inertial navigation system (INS) derived attitude error. The obtained $RMSE_r$ value is multiplied by a conversion factor of 1.7308 to yield the horizontal component of the National Standards for Spatial Data Accuracy (NSSDA) reporting standard where a theoretical point will fall within the obtained radius 95 percent of the time. Based on a flying altitude of 400 meters, an IMU error of 0.002 decimal degrees, and a GNSS positional error of 0.019 meters, this project was produced to meet 0.054 meters (0.178 feet) horizontal accuracy at the 95% confidence level. Table 19 provides the results at each flying height based on the acquisitions at 400, 600, and 2532 meters.

Table 19: Horizontal accuracy results.

Parameter	Horizontal Accuracy At 400 m Altitude	Horizontal Accuracy At 600 m Altitude	Horizontal Accuracy At 2532 m Altitude
$RMSE_r$	0.103 ft 0.031 m	0.042 ft 0.138 m	0.523 ft 0.159 m
ACC_r	0.178 ft 0.054 m	0.239 ft 0.073 m	0.904 ft 0.276 m

Digital Imagery Accuracy Assessment

This data set was tested as required by ASPRS Positional Accuracy Standards for Digital Geospatial Data, Edition 2 (2023). Although the Standards call for a minimum of thirty (30) checkpoints, this test was performed using only two (2) checkpoints. This data was produced to meet a 30 cm $RMSE_H$ horizontal positional accuracy class. The tested horizontal positional accuracy was found to be $RMSE_H$ = 5.5 cm using the reduced number of checkpoints.

Table 20 presents the complete photo accuracy statistics.

Table 20: Orthophotography accuracy statistics for Putah Creek

Parameter	Check Points$_x$	Check Points$_y$	Check Points$_h$	Control Points$_x$	Control Points$_y$	Control Points$_h$
		n=2			n=5	
Average	-0.037 ft -0.011 m	0.115 ft 0.035 m	0.063 ft 0.019 m	0.016 ft 0.005 m	0.007 ft 0.002 m	0.017 ft 0.005 m
RMSE	0.063 ft 0.019 m	0.170 ft 0.052 m	0.181 ft 0.055 m	0.078 ft 0.024 m	0.054 ft 0.016 m	0.095 ft 0.029 m
Standard Deviation (1σ)	0.074 ft 0.023 m	0.177 ft 0.054 m	0.192 ft 0.058 m	0.085 ft 0.026 m	0.006 ft 0.018 m	0.104 ft 0.032 m
1.96σ	0.146 ft 0.044 m	0.346 ft 0.106 m	0.376 ft 0.115 m	0.167 ft 0.051 m	0.118 ft 0.036 m	0.204 ft 0.062 m
Max Error	0.015 ft 0.005 m	0.240 ft 0.073 m	0.240 ft 0.073 m	0.110 ft 0.034 m	0.110 ft 0.034 m	0.156 ft 0.047 m
Min Error	-0.090 ft -0.027 m	-0.010 ft -0.003 m	-0.091 ft -0.028 m	-0.080 ft -0.024 m	-0.040 ft -0.012 m	-0.089 ft -0.027 m

CERTIFICATIONS

NV5 provided lidar services for the Putah Creek project as described in this report.

I, Jason Stuckey, have reviewed the attached report for completeness and hereby state that it is a complete and accurate report of this project.

Jason Stuckey
Jason Stuckey (May 16, 2025 12:00 AKDT) 05/16/2025

Jason Stuckey
Project Manager
NV5

I, Evon Silvia, PLS, being duly registered as a Professional Land Surveyor in and by the state of California, hereby certify that the methodologies, static GNSS occupations used during airborne flights, and ground survey point collection were performed using commonly accepted Standard Practices. Field work conducted for this report was conducted between January 28 - 30, 2025 and on February 27, 2025.

Accuracy statistics shown in the Accuracy Section of this Report have been reviewed by me and found to meet the "National Standard for Spatial Data Accuracy".

Evon P. Silvia 05/16/2025

Evon Silvia, PLS
NV5

Signed: 05/16/2025

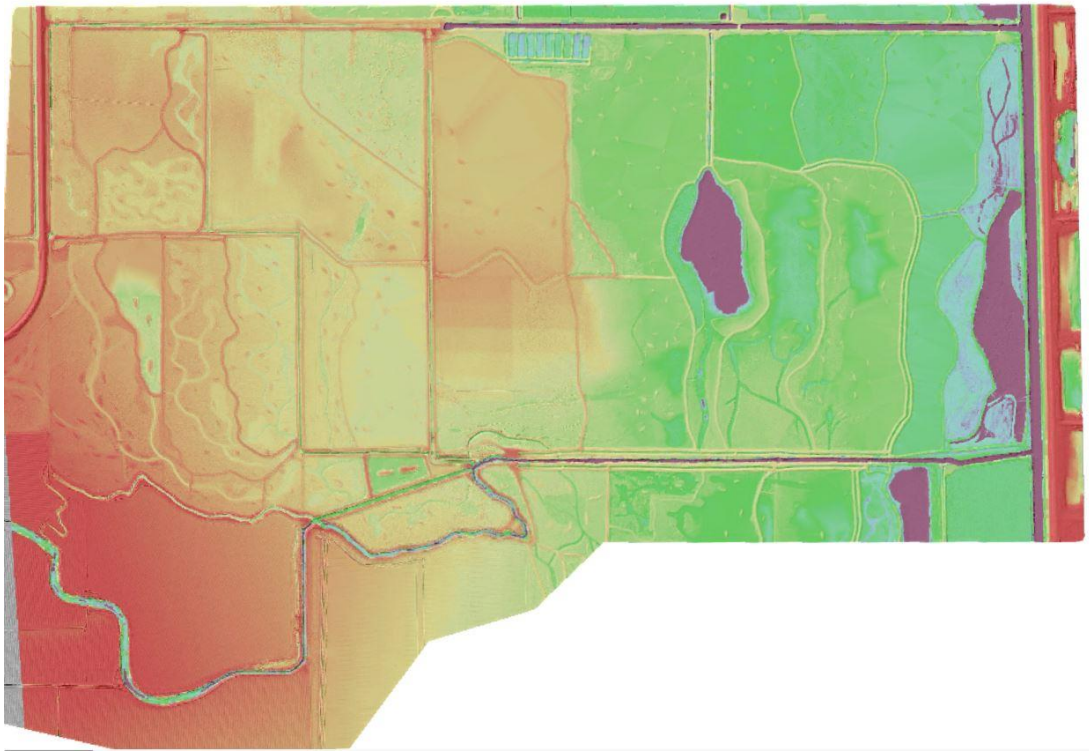

Figure 21: A nadir view oriented northward overlooking the Yolo Bypass Wildlife Area. The 3D image was created from the lidar bare earth model with color symbolizing elevation.

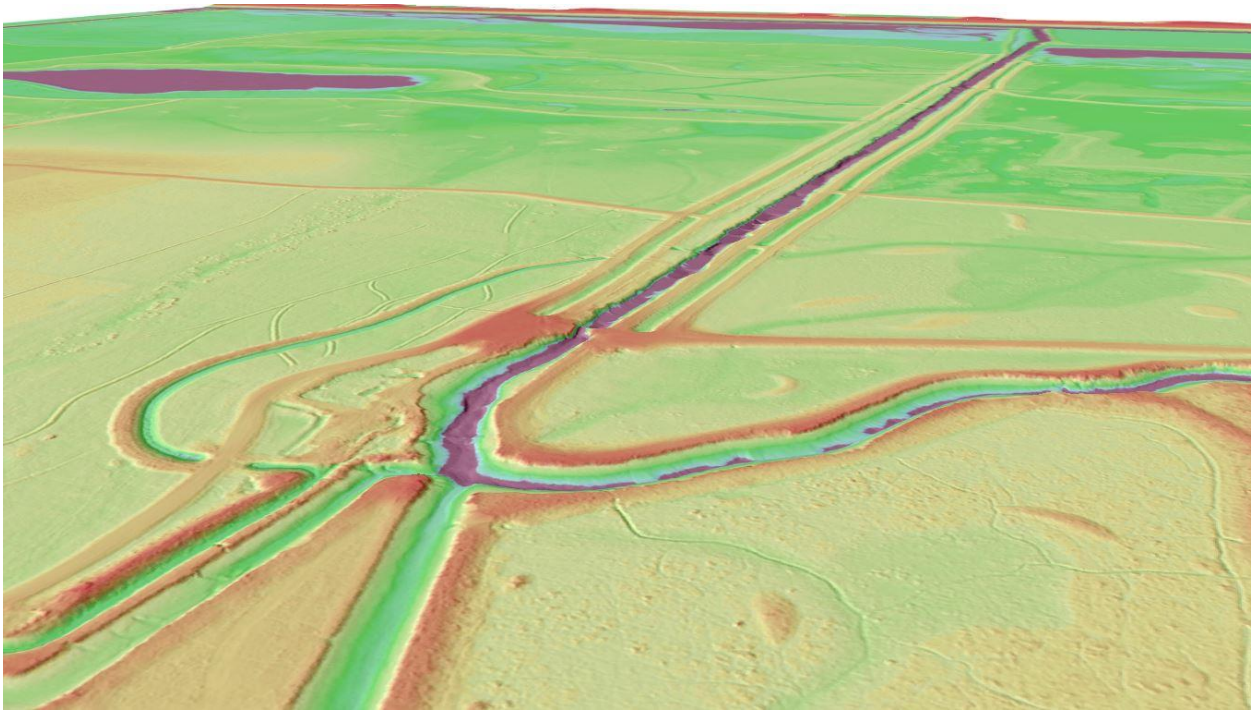

Figure 22: An oblique view looking northwest towards the Yolo Bypass Wildlife Area. The 3D image was created from the lidar bare earth model with color symbolizing elevation.

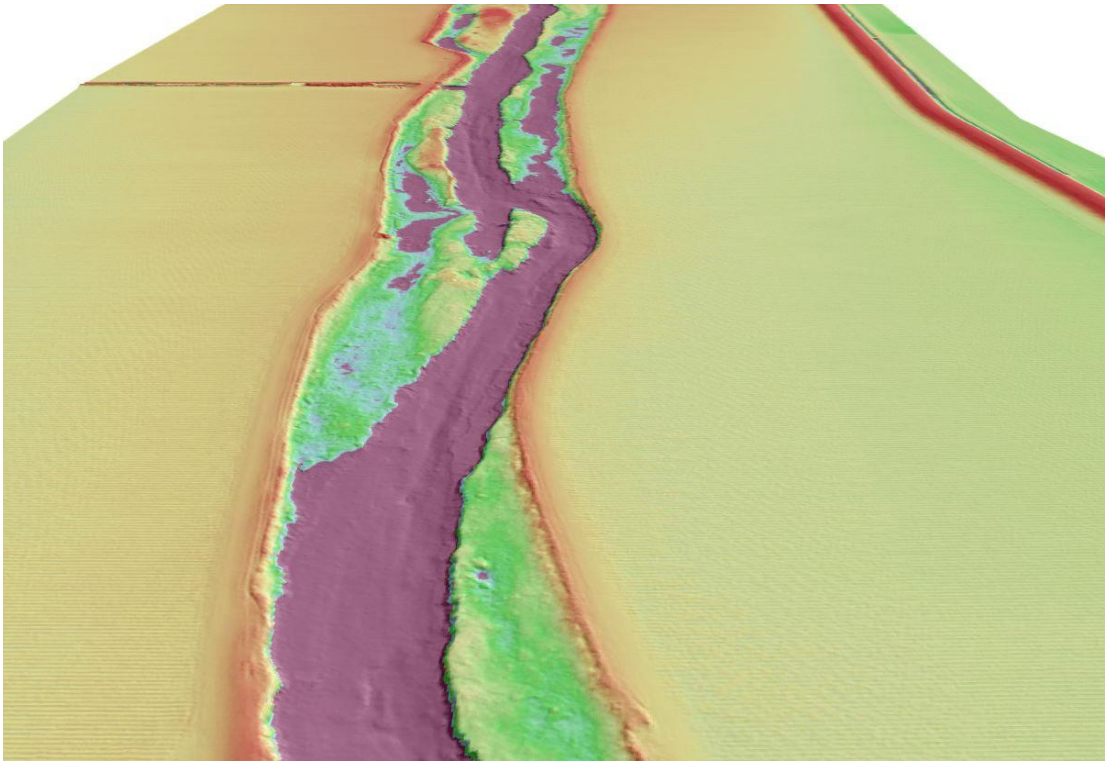

Figure 23: An oblique view looking west from an area just upstream of County Road 106A. The 3D image was created from the lidar bare earth model with color symbolizing elevation.

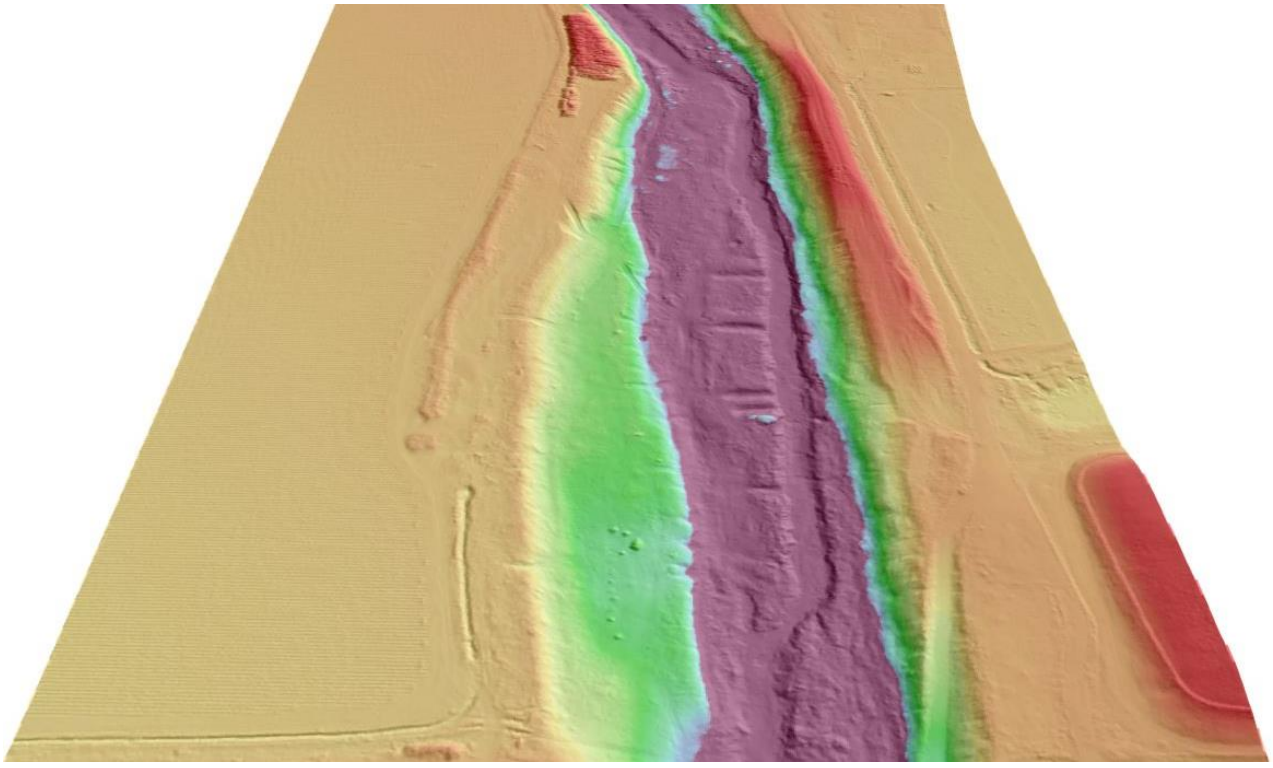

Figure 24: An oblique view looking west from an area just west of County Road 98. The 3D image was created from the lidar bare earth model with color symbolizing elevation.

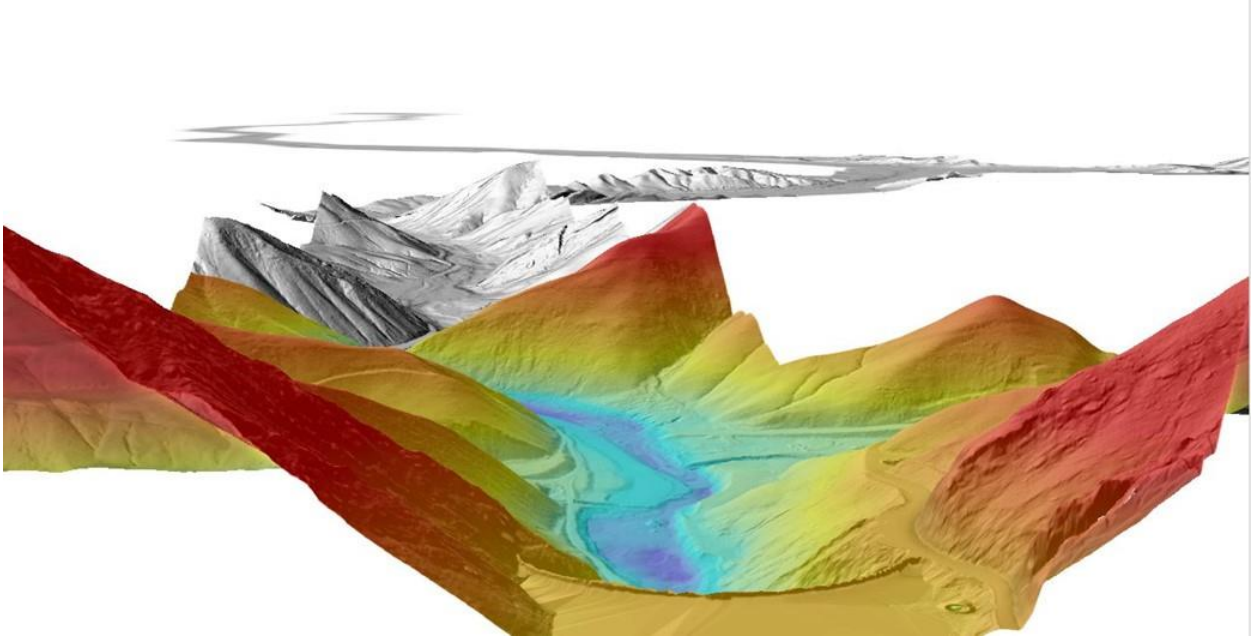

Figure 25: An oblique view looking east over the Monticello Dam and down the Putah Creek in California. The 3D image was created from the lidar bare earth model with a selected area symbolized and colored by elevation.

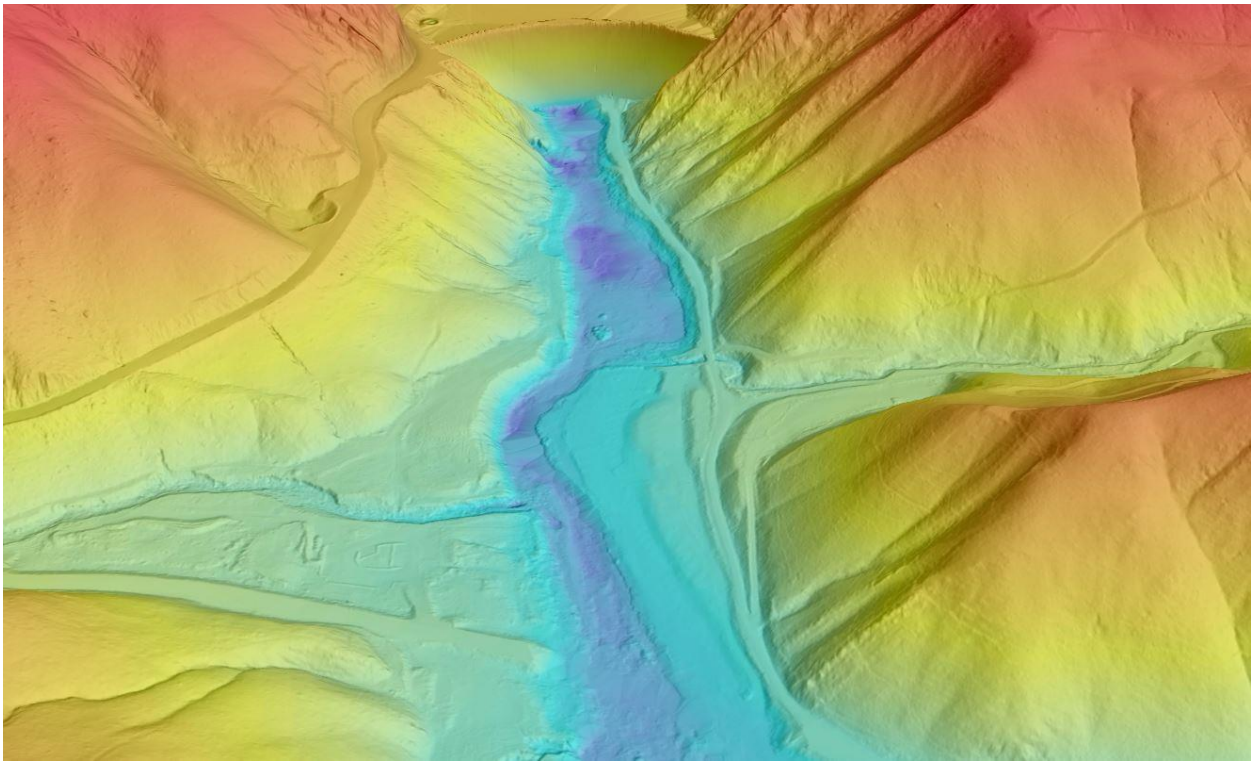

Figure 26: An oblique view looking west towards the Monticello Dam. The 3D image was created from the lidar bare earth model with color symbolizing elevation.

GLOSSARY

1-sigma (σ) Absolute Deviation: Value for which the data are within one standard deviation (approximately 68th percentile) of a normally distributed data set.

1.96 * RMSE Absolute Deviation: Value for which the data are within two standard deviations (approximately 95th percentile) of a normally distributed data set, based on the FGDC standards for Non-vegetated Vertical Accuracy (NVA) reporting.

Accuracy: The statistical comparison between known (surveyed) points and laser points. Typically measured as the standard deviation (sigma σ) and root mean square error (RMSE).

> **Absolute Accuracy:** The vertical accuracy of lidar data is described as the mean and standard deviation (sigma σ) of divergence of lidar point coordinates from ground survey point coordinates. To provide a sense of the model predictive power of the dataset, the root mean square error (RMSE) for vertical accuracy is also provided. These statistics assume the error distributions for x, y and z are normally distributed, and thus we also consider the skew and kurtosis of distributions when evaluating error statistics.
>
> **Relative Accuracy:** Relative accuracy refers to the internal consistency of the data set; i.e., the ability to place a laser point in the same location over multiple flight lines, GPS conditions and aircraft attitudes. Affected by system attitude offsets, scale and GPS/IMU drift, internal consistency is measured as the divergence between points from different flight lines within an overlapping area. Divergence is most apparent when flight lines are opposing. When the lidar system is well calibrated, the line-to-line divergence is low (<10 cm).
>
> **Root Mean Square Error (RMSE):** A statistic used to approximate the difference between real-world points and the lidar points. It is calculated by squaring all the values, then taking the average of the squares and taking the square root of the average.

Data Density: A common measure of lidar resolution, measured as points per square meter.

Digital Elevation Model (DEM): File or database made from surveyed points, containing elevation points over a contiguous area. Digital terrain models (DTM) and digital surface models (DSM) are types of DEMs. DTMs consist solely of the bare earth surface (ground points), while DSMs include information about all surfaces, including vegetation and man-made structures.

Intensity Values: The peak power ratio of the laser return to the emitted laser, calculated as a function of surface reflectivity.

Nadir: A single point or locus of points on the surface of the earth directly below a sensor as it progresses along its flight line.

Overlap: The area shared between flight lines, typically measured in percent. 100% overlap is essential to ensure complete coverage and reduce laser shadows.

Pulse Rate (PR): The rate at which laser pulses are emitted from the sensor; typically measured in thousands of pulses per second (kHz).

Pulse Returns: For every laser pulse emitted, the number of wave forms (i.e., echoes) reflected back to the sensor. Portions of the wave form that return first are the highest element in multi-tiered surfaces such as vegetation. Portions of the wave form that return last are the lowest element in multi-tiered surfaces.

Real-Time Kinematic (RTK) Survey: A type of surveying conducted with a GPS base station deployed over a known monument with a radio connection to a GPS rover. Both the base station and rover receive differential GPS data and the baseline correction is solved between the two. This type of ground survey is accurate to 1.5 cm or less.

Post-Processed Kinematic (PPK) Survey: GPS surveying is conducted with a GPS rover collecting concurrently with a GPS base station set up over a known monument. Differential corrections and precisions for the GNSS baselines are computed and applied after the fact during processing. This type of ground survey is accurate to 1.5 cm or less.

Scan Angle: The angle from nadir to the edge of the scan, measured in degrees. Laser point accuracy typically decreases as scan angles increase.

Native Lidar Density: The number of pulses emitted by the lidar system, commonly expressed as pulses per square meter.

Relative Accuracy Calibration Methodology:

Manual System Calibration: Calibration procedures for each mission require solving geometric relationships that relate measured swath-to-swath deviations to misalignments of system attitude parameters. Corrected scale, pitch, roll and heading offsets were calculated and applied to resolve misalignments. The raw divergence between lines was computed after the manual calibration was completed and reported for each survey area.

Automated Attitude Calibration: All data was tested and calibrated using TerraMatch automated sampling routines. Ground points were classified for each individual flight line and used for line-to-line testing. System misalignment offsets (pitch, roll and heading) and scale were solved for each individual mission and applied to respective mission datasets. The data from each mission were then blended when imported together to form the entire area of interest.

Automated Z Calibration: Ground points per line were used to calculate the vertical divergence between lines caused by vertical GPS drift. Automated Z calibration was the final step employed for relative accuracy calibration.

Lidar accuracy error sources and solutions:

Source	Type	Post Processing Solution
Long Base Lines	GPS	None
Poor Satellite Constellation	GPS	None
Poor Antenna Visibility	GPS	Reduce Visibility Mask
Poor System Calibration	System	Recalibrate IMU and sensor offsets/settings
Inaccurate System	System	None
Poor Laser Timing	Laser Noise	None
Poor Laser Reception	Laser Noise	None
Poor Laser Power	Laser Noise	None
Irregular Laser Shape	Laser Noise	None

Operational measures taken to improve relative accuracy:

Focus Laser Power at narrow beam footprint: A laser return must be received by the system above a power threshold to accurately record a measurement. The strength of the laser return (i.e., intensity) is a function of laser emission power, laser footprint, flight altitude and the reflectivity of the target. While surface reflectivity cannot be controlled, laser power can be increased and low flight altitudes can be maintained.

Reduced Scan Angle: Edge-of-scan data can become inaccurate. The scan angle was reduced to a maximum of ±29.25° from nadir, creating a narrow swath width and greatly reducing laser shadows from trees and buildings.

Quality GPS: Flights took place during optimal GPS conditions (e.g., 6 or more satellites and PDOP [Position Dilution of Precision] less than 3.0). Before each flight, the PDOP was determined for the survey day.

Ground Survey: Ground survey point accuracy (<1.5 cm RMSE) occurs during optimal PDOP ranges and targets a minimal baseline distance of 4 miles between GPS rover and base. Robust statistics are, in part, a function of sample size (n) and distribution. Ground survey points are distributed to the extent possible throughout multiple flight lines and across the survey area.

50% Side-Lap (100% Overlap): Overlapping areas are optimized for relative accuracy testing. Laser shadowing is minimized to help increase target acquisition from multiple scan angles. Ideally, with a 50% side-lap, the nadir portion of one flight line coincides with the swath edge portion of overlapping flight lines. A minimum of 50% side-lap with terrain-followed acquisition prevents data gaps.

Opposing Flight Lines: All overlapping flight lines have opposing directions. Pitch, roll and heading errors are amplified by a factor of two relative to the adjacent flight line(s), making misalignments easier to detect and resolve.